Electronic Journal of Biotechnology 73 (2025) 1–17

Contents lists available at ScienceDirect

Electronic Journal of Biotechnology

journal homepage: www.elsevier.com/locate/ejbt

Research article

Evaluation of high-value bioproducts production by marine endophytic fungus *Arthrinium* sp. FAKSA 10 under solid state fermentation using agro-industrial wastes ☆

Mohammad J. Alsarraf [a], Fuad Ameen [b,*], Abdullah Alfalih [b], Zirak Sajjad [c]

[a] Department of Science, College of Basic Education, The Public Authority of Applied Education and Training, Safat, Kuwait
[b] Department of Botany & Microbiology, College of Science, King Saud University, Riyadh, Saudi Arabia
[c] College of Human Medicine, Michigan State University, East Lansing, USA

GRAPHICAL ABSTRACT

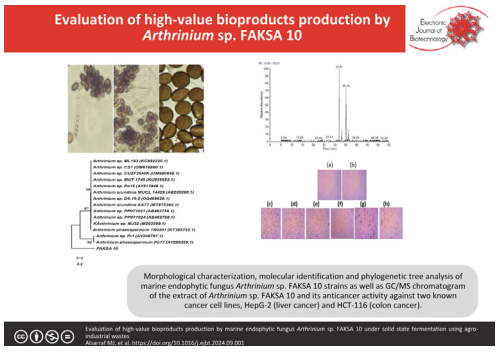

Evaluation of high-value bioproducts production by *Arthrinium* sp. FAKSA 10

ARTICLE INFO

Article history:
Received 1 August 2024
Accepted 12 September 2024
Available online 19 October 2024

Keywords:
Agro-industrial wastes
Anticancer enzymes
Anti-HCV
Antimicrobial
Antioxidant
Arthrinium sp.
Bioactive metabolites
Bioproducts
Endophytic fungi

ABSTRACT

Background: To address public health challenges, there is increasing interest in bioactive metabolites from unconventional sources for targeted cancer and viral treatments with minimal side effects. Endophytic fungi are promising for these therapies. This study focused on maximizing bioactive agent yields from these fungi using a low-cost medium and optimized fermentation system.

Results: Forty-three endophytic fungi isolated from *Sinularia polydactyla* were cultivated on wheat bran medium and evaluated for bioactive metabolites under solid-state fermentation. Strain FAKSA 10, identified as *Arthrinium* sp. FAKSA 10, exhibited the highest levels of pharmaceutical metabolites, including L-glutaminase, L-methioninase, L-arginase, L-asparaginase, L-tyrosinase, L-lysine α-oxidase, and ribonuclease, with a 79.12% hepatitis C virus knockdown rate. This strain produced 46 metabolites with anticancer, antioxidant, antiviral, and cytotoxic properties, including major compounds like hexadecanoic acid methyl ester; hexadecanoic acid ethyl ester; 9, 12-octadecadienoic acid (Z, Z), methyl ester; 9-octadecenoic acid (Z)-, methyl ester, and 11, 14-eicosadienoic acid, methyl ester. A cost-effective strategy using 11 agro-industrial residues was applied, followed by optimization of the solid-state fermentation system. This optimization increased enzyme yields and enhanced antiviral and antioxidant activities.

☆ Audio abstract available in Supplementary material.

Peer review under responsibility of Pontificia Universidad Católica de Valparaíso

* Corresponding author.
E-mail addresses: fuadameen@ksu.edu.sa (F. Ameen), sajjadzi@msu.edu (Z. Sajjad).

https://doi.org/10.1016/j.ejbt.2024.09.001

Marine fungus
Solid state fermentation

The optimal conditions for solid-state fermentation were a 10 d incubation, 1 mm particle size, 60% initial moisture, 28 °C temperature, and 2 × 10^7 CFU/mL inoculum size.
Conclusions: This study exploited *Arthrinium* sp. FAKSA 10 metabolites as natural pharmaceuticals against cancer and viral diseases, highlighting their significant antioxidant properties. Among various residues, oil cakes emerged as an effective and cost-efficient medium, capable of significantly enhancing the production of valuable bioactive metabolites.
How to cite: Alsarraf MJ, Ameen F, Alfalih A, et al. Evaluation of high-value bioproducts production by marine endophytic fungus *Arthrinium* sp. FAKSA 10 under solid state fermentation using agro-industrial wastes. Electron J Biotechnol 2025;73. https://doi.org/10.1016/j.ejbt.2024.09.001.

1. Introduction

Cancer is indeed a significant global health concern, leading to millions of deaths annually and prompting extensive research efforts. Overall, Asia, Africa, and America account for 70% of all cancer fatalities and 60% of all cancer cases recorded worldwide. [1,2]. Chronic hepatitis C virus (HCV) infection also presents a major public health challenge, with approximately 71 million people infected universally and about 1.0 million new infections arising every year [3]. In Saudi Arabia, the incidence of HCV is approximately 0.7%, and about 70% of these infected individuals having active infection individuals having active infection [4]. Uncontrolled reactive oxygen species (ROS) or free radicals can actually lead to systemic oxidative stresses, which are implicated in damaging biological macromolecules and managing their levels and maintaining antioxidant defenses are crucial in supporting overall health and longevity [5]. This oxidative damage contributes to a range of debilitating conditions including cancer, neurodegenerative disorders, and diabetes, and accelerates the aging process. Additionally, ROS can promote lipid peroxidation, impair innate antioxidant enzymes, and disrupt normal metabolic functions, further exacerbating cellular damage and metabolic disorders [6].

In addressing these public health challenges, there is a growing demand for unconventional sources of bioactive metabolites sought for their potential to offer high specificity in targeting cancer and viral diseases with minimizing side effects [7]. In this regard, the exploration of endophytic fungi for bioactive metabolites represents a promising avenue for developing new therapies [8]. Furthermore, their ability to produce compounds with specific activity against cancer cells and viruses provides opportunities for developing new therapies with potentially fewer side effects compared to conventional treatments to address current healthcare gaps [9]. RNases, enzymes that degrade viral genomes, are considered promising candidates for broad-spectrum antiviral therapeutics because of their unique ability to hydrolyze nucleic acids [10]. Fungal RNases have demonstrated efficacy against RNA viral pathogens through a multifaceted approach including enzymatically targeting the viral genome [11].

Among endophytes, marine coral-endophytic fungi are recognized as a significant component of the endophytic microbiota, offering a wealth of therapeutic agents with anticancer, antioxidant, and antiviral activities [9,12]. Recently, endophytic fungi have emerged as a promising source for enzymatic amino acid deprivation therapies in cancer treatment; these therapies aim to deprive auxotrophic cancer cells of essential nutrients [13]. These enzymes including asparaginases, arginine deiminases, arginases, methioninases, lysine oxidases, phenylalanine ammonia lyases, and glutaminases have recently been developed for their anticancer, antioxidant, antimicrobial, and anti-HCV properties [9,14,15,16]. Globally *Arthrinium* species have been commonly isolated as endophytes with promising broad-spectrum bioactive agents including enzymatic, antimicrobial, antioxidant, anticancer and antiviral agents [17].

The great cost of conventional antioxidant, anti-HCV, anticancer and antimicrobial drugs is a burden for nations, there is an urgent necessity to develop an environmentally safe technology along with cost-effective strategies such as solid-state fermentation system for the production of pharmaceutical bioactive agents, and some of them may exhibit pronounced antioxidant, anticancer, and antiviral activities while some others can exert antibiotic as well as pharmaceutical enzymatic activities [18,19]. After processing of fruits, vegetables and oils, various agroindustrial residues (seeds, peels, whole pomace or oil cakes) contain soluble sugars, fibers, and other hydrolyzable materials and can be metabolized in solid state fermentation (SSF) by a wide range of fungi via fermentation into several value-added bioactive products [20,21]. Almost every marine-derived *Arthrinium* species demonstrated high antioxidant activity in radical-scavenging assays. Notably, the crude extract of *Arthrinium* sp. 3 KUC21327 displayed higher radical-scavenging activity than ascorbic acid [22].

Therefore, the current study aimed to obtain endophytic fungi that produce maximum yields of appreciated pharmaceutical products, comprising enzymes such as L-lysine α-oxidase, L-tyrosinase, L-methioninase, L-arginase, L-asparaginase, L-glutaminase, and RNase. Additionally, the study focused on evaluating the antioxidant, antiproliferative, and antiviral activity targeting hepatitis C virus, using a low-cost production medium under an optimized solid-state fermentation system.

2. Materials and methods

2.1. Isolation of coral-endophytic fungi

Samples of the coral *Sinularia polydactyla* were obtained from Sharm Abḥur (between latitudes 21°42′11″ and 21°45′24″ and longitudes 39°05′12″ and 39°08′48″E), Jeddah coast, Mecca Region, eastern side of the Red Sea, Saudi Arabia (Fig. 1) in March 2022. Coral samples were washed with seawater, preserved in polythene bags with seawater, and transported to the laboratory in a container filled with ice for isolation of endophytic mycobiome by the surface sterilization method [23]. The coral specimens underwent a 5-min wash in running water followed by being cut into small fragments (1.0 × 0.5 cm). These pieces were then sterilized by immersing them in 70% ethanol for 3 min, followed by 2.0% sodium hypochlorite for 2 min, and another round of 70% ethanol for 2 min. After sterilization, the pieces were rinsed in sterile water for 2 min before being inoculated (10 pieces/plate) onto MYPGA medium plates. The plates were then incubated at 28°C for 2 weeks, with regular monitoring till colonies appeared from the inner tissues of coral. Pure fungal colonies were maintained on MYPGA.

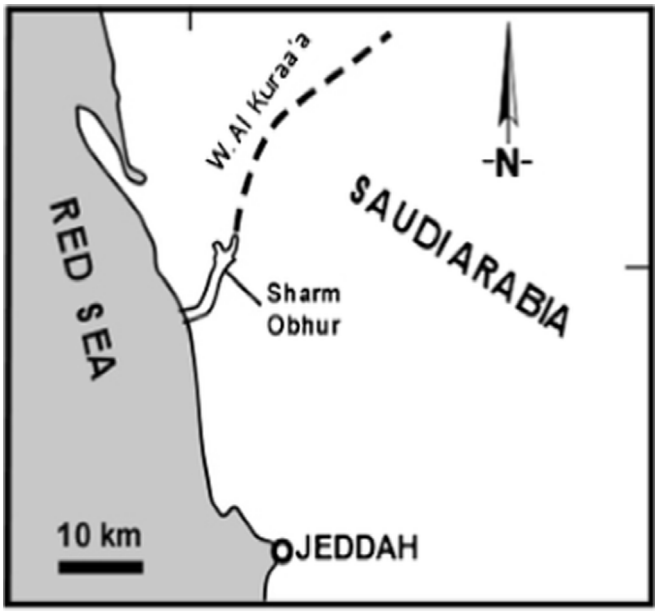

Fig. 1. Sampling site of the Soft coral *Sinularia polydactyla* at Sharm Abhur, eastern side of the Saudi Red Sea Coast, Saudi Arabia.

2.2. Fungal growth

Two discs, each 2 cm in diameter from an established culture of the tested fungi were inoculated into 500 mL Erlenmeyer flasks (5 flasks/isolate) containing 5 g of wheat bran sized to 2 mm with initial moisture content adjusted to 60% at pH 6.0 and incubated at 28°C for 10 d.

2.3. Enzymes extraction

To extract enzymes from SSF cultures, a known amount of wheat bran culture for each isolate was mixed well and extracted with distilled water (1:3 w/v) containing 0.1% Tween-80 for 2 h at 30°C and 180 rpm. Suspensions were then filtrated through Whatman filter paper No. 1 followed by centrifugation at 8,000 rpm for 10 min at 4°C, and the supernatants were used for enzyme assays. The yield of each enzyme was expressed as the total units of enzyme achieved per gram of dry substrate (U/gds).

2.4. Assays of pharmaceutical enzymes

L-Methioninase, L-glutaminase, and L-asparaginase activity were measured using L-methionine, L-glutamin, and L-asparagine as substrates, respectively, following the nesslerization method. Liberated ammonia was estimated at 425, 450, and 450 nm using a UV–Visible spectrophotometer (Shimadzu, Kyoto, Japan) for L-methioninase, L-glutaminase, and L-asparaginase activity, respectively [12,20]. One unit of each enzyme was defined as the amount of enzyme catalyzed in the release of 1 μmol of ammonia/min under standard assay conditions.

Tyrosinase activity was assayed using L-tyrosine as substrate, and the absorbance was monitored at 475 nm. One unit of tyrosinase was defined as the amount of enzyme catalyzed in the formation of 1 μmol of L-dopachrome/min [24]. L-Arginase activity was quantified using L-arginine as substrate, and the liberated urea was measured at 540 nm as described by Nadaf et al. [14]. Enzyme activity (U/mL) was calculated as μmoles of urea released/min/mL [14]. L-Lysine α-oxidase activity was calculated by the forming rate of H_2O_2 in a 20 mM Tris-phosphate buffer (pH 7.8) containing 0.2 mM o-dianisidine, 5 μg/mL peroxidase, and 2.0 mM L-lysine at 25°C. One unit of the enzyme was calculated as the amount of enzyme that catalyzes the oxidation of 1 μmoL L-lysine/min [15]. RNase activity was determined using tRNA as the substrate as described by Wu et al. [25]. One unit of RNase is defined as the amount of enzyme that increases OD_{260} of one/min/mL of reaction mixture under standard assay conditions [25].

2.5. Extraction of bioactive metabolites for anti-HCV, antioxidant and anticancer activities

To determining antiviral, antioxidant and antimicrobial activities, a known number of whole cultures were extracted twice with methanol (1:3 w/v), dried under vacuum, weighted and tested for antiviral, antioxidant, anticancer and antibacterial activity.

2.6. Anti-hepatitis C virus

Murine MH1 cells were utilized to assess the effectiveness of substances extracted from 43 fungal isolates cultured on wheat bran medium, as well as the efficiency of the extracted metabolites from the selected strain FAKSA 10 grown on eleven agro-industrial residues in inhibiting the hepatitis C virus (HCV). Cells were maintained and cultured in Dulbecco's modified Eagle medium (DMEM) containing 100 IU/mL penicillin G sodium and streptomycin sulfates, 1% of L-glutamine and 10% fetal bovine serum at 37°C in incubator at 5% CO_2, and then, assessments were done in the logarithmic growth phase. Each extract was dissolved in DMSO, and cells were seeded at density 4×10^4/well and were treated with 80 μg/mL of tested extracts, individually at 37°C for 48 h. Likewise, the extract of the selected strain FAKSA 10 on different agroindustrial residue-based media at different concentrations was evaluated for their anti-HCV, and then, the half inhibition concentrations (IC_{50}) were determined [26].

2.7. Gas chromatography-mass spectrometry (GC-MS) analyses of FAKSA 10 extract of wheat bran culture

Wheat bran medium was inoculating the wheat bran with the FAKSA 10 fungal strain. The inoculated wheat bran was incubated under controlled conditions for a specified period mentioned above to allow the fungi to grow and produce metabolites. The fungal biomass was extracted using methanol to extract the fungal metabolites, followed by filtration, centrifugation and concentration of the extract using a rotary evaporator. The concentrated extract was dissolved in dichloromethane and filtered to remove any particulate matter. Two μL of extract was injected, individually into the GC-MS instrument. The sample is vaporized and carried by an inert gas (helium) through a chromatographic column (TG-5MS fused silica capillary column), at a flow rate of one mL/min and temperature set at 280°C. Compounds get separated based on its volatility and interaction with the column's stationary phase. As the separated compounds elute from the GC column, they are ionized at an ionization energy of 70 eV and fragmented in the mass spectrometer. The mass spectrometer detects the ions and generates a mass spectrum for each compound. The mass spectra and retention times of the detected compounds were compared with those in a NIST and WILLY reference library to identify the metabolites.

2.8. Morphological, molecular and phylogeny characterization of the selected endophytic isolate FAKSA 10

The morphological characteristics of isolate FAKSA 10 were observed following two weeks of growth on malt extract agar

(MEA), oatmeal agar (OA), and potato dextrose agar (PDA) in the darkness at a temperature of 28°C. Culture characteristics including structure, colony color, mycelium, and diffusible pigments were recorded [27]. Micromorphological properties were examined and pictured by a compound microscope (Nikon Eclipse 80i) equipped with a digital camera (Canon 450D). All measurements of microscopic details including conidiophore length, conidiogenous cell dimensions, and conidial characteristics were performed using Tarosoft Image Framework (v. 0.9.0.7). The morphological characteristics of the selected isolate FAKSA 10 were performed as previously described [17,28,29,30,31].

For molecular analysis, DNA was extracted from the strain FAKSA 10 by the QIAamp DNA Mini Kit (Qiagen, Inc., Valencia CA), following the manufacturer's instructions. The extracted DNA was examined using a spectrophotometer. The ITS1 (5′-TCC GTAGGTGAACCTGCGG-3′) and ITS4 (5′-TCCTCCGCTTATTGA TATGC-3′) universal primer pairs were utilized to amplify the ITS1-5.8S-ITS2 region [32]. The PCR amplification product was purified using the PCR Cleanup Kit (Qiagen Inc., Valencia, CA) and sequenced on an ABI 3730xl DNA sequencer using the Big Dye Terminator cycle sequencing kit (Applied Biosystems, Inc., Foster City, CA) [33]. The resultant sequences were matched to the GenBank database via the Basic Local Alignment Search Tool (BLAST) accessible at the National Center for Biotechnology Information (NCBI) (https://www.ncbi.nlm.nih.gov/BLAST/). Accordingly, the nucleotide sequence of the FAKSA 10 isolate was submitted to GenBank and gave an accession number. Phylogenetic analysis involved assembling, proofreading, and editing the ITS sequences using MEGA 11. The phylogenetic tree was built using the neighbor-joining method and evaluated through bootstrap analysis with MEGA 11 [34,35,36].

2.9. Optimization of SSF parameters

Proper fermentation optimization was examined using one factor at a time to test the factors for maximum yield, and then, the optimized factor was applied in the next experiment for each activity. Optimization of process parameters has been initiated using agro-industrial by-products as cheap substrates for producing wide-ranging bioactive metabolites like pharmaceutical enzymes, antioxidants, antiviral and anti-tumor activities. A total of eleven natural agroindustrial residues including oil cakes of olive (OOC), palm (POC), wheat germ (WGC), sesame (SOC), almond (AOC), mustard (MOC), coconut (COC); peels of pomegranate (POP) and banana (BP); and brans of rice (RB) and wheat bran (WB) were obtained from local suppliers and screened for the production of these bioactive metabolites. WB culture was considered as control. They were washed, sliced into small species, desiccated in an oven at 50°C to reach constant weight, and then, they were powdered and sized to 2.0 mm and then, each one was evaluated as a production medium compared to WB. Five grams of each substrate were placed individually in a 250 mL Erlenmeyer flask, moistened with 60% deionized water, autoclaved, and allowed to cool. The cooled substrates were then inoculated with strain FAKSA 10 (2×10^6 CFU/gds), carefully mixed, and incubated at 28°C for 10 d. For anti-HCV, antioxidant, and anticancer activities, the effect of fermentation media consisting of the best inducers OOC, SOC, AOC, and MOC was evaluated at ratios of (1:1:1:1), (2:1:1:1), (1:2:1:1), (1:1:2:1), and (1:1:1:2), respectively. Following incubation, bioactive metabolites were extracted twice in methanol (1:5 w/v). Various parameters in the SSF system were optimized to maximize the yields of bioactive metabolites at the lowest production cost. These parameters were incubation period (5, 7, 10, 14, and 20 d), particle size (0.5, 1.0, 2.0, 4.0, and 6.0 mm), initial moisture content (50, 60, 70, 80, and 90% v/w), incubation temperature (25–45°C), and inoculum size (2×10^6, 2×10^7 and 2×10^8 CFU/gds).

2.10. Cytotoxicity assessment and determination of the half inhibitory concentration (IC_{50}) values

Hepatocellular carcinoma (HepG-2), normal lung WI-38 and colon cancer HCT-116 cell lines were maintained in RPMI 1640 medium (Gibco) accompanied with 10% heat-inactivated fetal bovine serum, streptomycin and penicillin at 100 U/mL and incubated at 37°C in a humidified 5% CO_2 atmosphere. The cytotoxic properties and IC_{50} values of extracts obtained from fungi grown on various waste-based culture media mentioned earlier were evaluated against HepG-2, HCT-116, and WI-38 cells using the MTT [(3, 4, 5, dimethyl thiazol-2-yl)-2,5-diphenyl tetrazolium bromide] cytotoxic assay [37] at the National Research Centre. Cells were plated in 96-well plates at a density of 1×10^4 cells/well and incubated for 48 h before being exposed to each extract or the reference drug doxorubicin at a concentration that ranged from 0 to 150 μg/mL for cancerous cells and ranged from 100 to 1000 μg/mL for normal cell line. Next, cells were incubated with 1 mg/mL MTT reagent at 37°C for 3 h, followed by removal of the reagent. The mitochondrial succinate dehydrogenase and reductase enzymes in live cells changed MTT to a quantifiable purple formazan product, which relates with the number of viable cells and inversely correlates with cytotoxicity. Formazan crystals were dissolved with 100 mL of DMSO and estimated colorimetrically at absorbance A_{540} nm by the microplate reader. Cell viability (%) was quantified according to [**Equation 1**]:

$$\text{Cells viability}\,(\%) = \frac{A_{\text{test}} - A_{\text{blank}}}{A_{\text{control}} - A_{\text{blank}}} \times 100 \quad (1)$$

where A_{test}, $A_{Blank\ and}$ $A_{control}$ are the OD_{540} nm of treated cells, culture medium, and control cells, respectively. IC_{50} of each treatment was determined from the concentration–response curve where the extract decreased cell viability by 50% compared to untreated cells. All experiments were conducted in triplicate.

2.11. Antioxidant activities

2.11.1. DPPH radical scavenging assay

The capability of the extracts for scavenging free radicals was evaluated using the DPPH radical scavenging assay as seen in [**Equation 2**] [38]. In this assay, DPPH altered from violet to yellow in the existence of antioxidants. Each test extract (100 μL) at concentrations ranging from 0 to 150 μg/mL was carefully mixed with 100 μL of DPPH reagent (0.2 mg/mL in MeOH), and incubated at 28°C in the dark for 30 min. Absorbance was measured at λ = 515 nm.

$$\text{DPPH radical scavenging activity}\,(\%) = \frac{A_0 - A_1}{A_0} \times 100 \quad (2)$$

where A_0 and A_1 are the absorbance of control and tested extract, respectively. The inhibition percentages were plotted against concentrations to determine the amount of extract or standard needed for scavenging 50% of DPPH free radicals. Experiments were conducted in triplicate. Ascorbic acid (10–100 μg/mL) was served as standard.

2.11.2. Reducing power assay

The study involved adding 0.05 mL extract at various concentrations, 0 to 150 μg/mL, to a mixture containing 0.2 mL of 0.2 M phosphate buffer (pH 6.6) and 0.2 mL of 1% potassium ferricyanide, incubated at 50°C for 20 min, adding 0.25 mL of trichloroacetic acid and then centrifuged at 1000 rpm for 15 min. 0.1 mL of 0.1% $FeCl_3$

was mixed with 5 mL of supernatant, and deionized water and absorbance was estimated at 700 nm to assess the reductive potential of the fungal extracts [39]. Ascorbic acid was used as a reference.

2.12. Statistical analysis

The results were statistically processed by analyses of variance (ANOVA), followed by Tukey's tests when significant effects were detected ($p \leq 0.05$). Data were expressed as means ± standard error.

3. Results and discussion

3.1. Screening of pharmaceutical enzyme activities of marine coral endophyte fungi using wheat bran medium

As shown in Table 1 all fungal isolates were potent producers for the enzymes L-lysine α-oxidase, L-methioninase, L-asparaginase and RNase while only 83.72% (n = 36), 69.77% (n = 30) and 81.39% (n = 35) of all fungal isolates (n = 43 isolates) were able to produce L-tyrosinase, L-glutaminase, and L-arginase, respectively. Appreciate amounts of L-lysine α-oxidase were detected in all strains but the highest yields were detected in FAKSA 10, FAKSA 5, FAKSA 25, FAKSA 6, FAKSA 19 and FAKSA 12 (132.53 ± 3.21, 129.00 ± 3.15, 120.70 ± 2.85, 118.46 ± 3.08, 117.54 ± 2.80 and 115.57 ± 3.09 U/gds), respectively (Table 1). L-lysine α-oxidase from fungi exhibits anticancer, antimicrobial, and antiviruses *in vivo* through exhaustion of the necessary amino acid L-lysine and achievement of reactive oxidative species formed in reaction [40]. Moreover, the fungal L-lysine α-oxidase produced by *Trichoderma harzianum* in cancer therapy targets and hydrolyzes L-lysine and then prompts apoptosis to and prevents cancer cell proliferation [7]. Maximum L-tyrosinase yield was obtained from isolate FAKSA 10 (97.12 ± 1.19 U/gds) followed by FAKSA 25, FAKSA 42, FAKSA 13, FAKSA 6 and FAKSA 23 (90.34 ± 1.25, 90.00 ± 1.32, 89.29 ± 1.18, 87.18 ± 1.10 and 82.99 ± 1.09 U/gds), respectively (Table 1). The production of tyrosinase is broadly distributed between microbial communities, and it is used to treat primary immune responses, skin-pigmentation, wound curing, Parkinson's, sarcomas and viral diseases besides its uses as cosmetics, drug carrier, and antioxidant compound [13]. On the other hand, Lopez-

Table 1
Screening of the soft coral – endophytic fungi for the production of anticancer and antiviral agents using wheat bran medium.

Isolate	Pharmaceutical enzymes productivity (U/gds)							Anti-HCV* VKD %
	L-Lysine α-oxidase	L-Tyrosinase	L-Methioninase	L-Glutaminase	L-Arginase	L-Asparaginase	RNase	
FAKSA 1	107.87 ± 2.89	ND	115.40 ± 1.16	190.34 ± 1.73	68.70 ± 1.08	115.26 ± 1.19	317.32 ± 1.59	−57.52
FAKSA 2	112.14 ± 3.01	21.19 ± 0.33	213.36 ± 2.18	227.00 ± 2.18	92.50 ± 1.46	159.80 ± 1.83	201.40 ± 0.91	−65.77
FAKSA 3	87.89 ± 2.34	50.42 ± 0.61	94.15 ± 1.00	110.11 ± 1.54	105.13 ± 1.85	131.46 ± 1.38	186.97 ± 1.16	−70.15
FAKSA 4	95.97 ± 2.52	74.13 ± 0.92	122.43 ± 1.25	ND	73.40 ± 1.12	89.44 ± 0.92	174.23 ± 1.35	−38.50
FAKSA 5	129.00 ± 3.15	69.27 ± 0.75	130.47 ± 1.36	117.43 ± 1.60	57.91 ± 0.97	95.56 ± 1.00	188.00 ± 1.52	−44.61
FAKSA 6	118.46 ± 3.08	87.18 ± 1.10	94.75 ± 1.03	80.40 ± 1.00	101.18 ± 1.80	156.30 ± 1.65	290.34 ± 1.25	−69.20
FAKSA 7	102.19 ± 2.82	ND	35.21 ± 0.24	70.38 ± 0.95	78.43 ± 1.19	88.50 ± 0.89	128.90 ± 1.40	−32.16
FAKSA 8	100.52 ± 2.84	75.40 ± 1.00	150.60 ± 1.50	ND	56.90 ± 0.98	117.92 ± 1.17	107.50 ± 1.73	−34.96
FAKSA 9	89.15 ± 2.40	25. 68 ± 0.36	23.50 ± 0.19	105.76 ± 1.50	ND	135.21 ± 1.64	139.14 ± 0.60	−50.50
FAKSA 10	132.53 ± 3.21	97.12 ± 1.19	242.70 ± 2.63	235.30 ± 2.11	146.93 ± 2.00	180.20 ± 1.85	325.16 ± 1.90	−79.12
FAKSA 11	75. 92 ± 2.27	43.50 ± 0.57	68.13 ± 0.56	ND	82.53 ± 1.36	40.30 ± 0.48	171.44 ± 1.29	−44.45
FAKSA 12	115.57 ± 3.09	69.43 ± 0.80	103.46 ± 1.05	ND	97.14 ± 1.60	130.30 ± 1.33	206.26 ± 1.65	−60.10
FAKSA 13	90.60 ± 2.40	89.29 ± 1.18	129.70 ± 1.40	182.19 ± 2.08	65.28 ± 1.02	144.80 ± 1.40	307.50 ± 1.57	−59.30
FAKSA 14	88.34 ± 2.42	81.22 ± 1.02	120.39 ± 1.06	120.55 ± 1.69	ND	138.50 ± 1.31	296.32 ± 1.35	−66.85
FAKSA 15	101.80 ± 2.69	28.40 ± 0.32	91.44 ± 1.12	50.25 ± 0.82	112.17 ± 1.95	60.28 ± 0.65	215.37 ± 0.97	−68.17
FAKSA 16	83.27 ± 2.35	43.98 ± 0.55	150.08 ± 1.51	205.43 ± 2.09	133.20 ± 2.30	81.32 ± 0.80	273.38 ± 1.65	−75.92
FAKSA 17	61.38 ± 2.00	65.11 ± 0.91	73.99 ± 0.74	113.80 ± 1.42	53.90 ± 0.80	139.40 ± 1.36	116.13 ± 1.13	−48.60
FAKSA 18	80.16 ± 2.27	ND	125.00 ± 1.36	27.33 ± 0.50	97.26 ± 1.90	101.60 ± 1.01	245.22 ± 1.55	−55.33
FAKSA 19	117.54 ± 2.80	70.50 ± 1.07	102.29 ± 1.03	ND	49.81 ± 0.72	65.30 ± 0.70	131.90 ± 0.49	−39.80
FAKSA 20	51.10 ± 1.69	52.18 ± 0.68	190.55 ± 1.87	100.76 ± 1.29	ND	50.80 ± 0.54	169.14 ± 1.20	−41.41
FAKSA 21	76.94 ± 2.40	68.30 ± 1.02	88.31 ± 0.80	65.96 ± 0.82	100.25 ± 1.81	106.45 ± 1.13	200.27 ± 1.26	−65.50
FAKSA 22	80.49 ± 2.33	ND	193.68 ± 1.90	ND	ND	142.15 ± 1.55	218.00 ± 0.95	−58.27
FAKSA 23	64.18 ± 2.11	82.99 ± 1.09	65.31 ± 0.73	116.24 ± 1.50	105.00 ± 1.72	137.24 ± 1.43	174.10 ± 1.29	−66.00
FAKSA 24	87.26 ± 2.41	28.60 ± 0.32	60.92 ± 0.68	31.60 ± 0.56	88.37 ± 1.54	160.27 ± 1.64	221.56 ± 0.47	−64.80
FAKSA 25	120.70 ± 2.85	90.34 ± 1.25	226.10 ± 2.13	214.65 ± 1.95	127.65 ± 1.97	171.68 ± 1.77	319.20 ± 1.85	−72.52
FAKSA 26	114.00 ± 2.70	59.13 ± 0.75	109.75 ± 1.10	160.50 ± 2.11	90.02 ± 1.03	63.90 ± 0.61	192.65 ± 1.52	−61.40
FAKSA 27	75.25 ± 2.40	60.28 ± 0.76	42.69 ± 0.40	41. 55 ± 0.53	ND	104.63 ± 1.01	118.74 ± 1.47	−39.18
FAKSA 28	110.36 ± 2.93	38.46 ± 0.43	125.35 ± 1.39	ND	48.31 ± 0.75	102.30 ± 1.06	146.31 ± 0.84	−38.90
FAKSA 29	45.28 ± 1.57	ND	99.40 ± 0.91	100.18 ± 1.32	40.27 ± 0.64	120.38 ± 1.23	191.28 ± 1.50	−41.34
FAKSA 30	90.22 ± 2.86	76.85 ± 1.24	134.71 ± 1.45	23.21 ± 0.45	93.50 ± 1.50	59.70 ± 0.52	265.35 ± 1.69	−60.16
FAKSA 31	65.22 ± 2.19	48.90 ± 0.61	62.88 ± 0.60	95.80 ± 1.12	ND	83.69 ± 0.85	200.05 ± 1.63	−36.21
FAKSA 32	79.08 ± 2.25	26.05 ± 0.38	115.00 ± 1.33	ND	62.15 ± 1.06	101.81 ± 1.08	150.79 ± 1.00	−49.15
FAKSA 33	102.19 ± 2.72	54.10 ± 0.63	89.42 ± 0.82	ND	43.62 ± 0.69	85.17 ± 0.90	170.25 ± 1.30	−45.10
FAKSA 34	69.53 ± 1.68	ND	199.35 ± 1.88	149.11 ± 1.77	74.32 ± 1.11	68.36 ± 0.69	169.82 ± 1.19	−56.29
FAKSA 35	75.92 ± 2.21	70.33 ± 0.98	174.85 ± 1.60	200.00 ± 2.05	119.65 ± 1.97	130.26 ± 1.35	237.59 ± 1.54	−71.00
FAKSA 36	104.98 ± 2.80	41.18 ± 0.55	160.63 ± 1.54	ND	80.15 ± 1.42	77.40 ± 0.80	139.70 ± 0.55	−64.97
FAKSA 37	79.21 ± 2.29	70.95 ± 1.06	62.80 ± 0.61	96.32 ± 1.16	32.79 ± 0.55	119.60 ± 1.22	183.25 ± 1.68	−38.52
FAKSA 38	81.28 ± 2.41	68.90 ± 1.01	117.83 ± 1.48	117.61 ± 1.52	ND	163.58 ± 1.71	196.18 ± 1.46	−47.15
FAKSA 39	102.90 ± 2.69	50.63 ± 0.67	50.75 ± 0.49	ND	71.30 ± 1.04	129.34 ± 1.33	284.20 ± 1.40	−38.17
FAKSA 40	100.02 ± 2.66	72.28 ± 1.09	183.08 ± 1.74	135.04 ± 1.78	103.27 ± 1.83	135.4 ± 1.46	185.72 ± 1.48	−65.96
FAKSA 41	50.35 ± 1.87	73.42 ± 1.15	98.51 ± 0.88	210.90 ± 2.12	69.18 ± 1.09	78.50 ± 0.93	213.09 ± 1.07	−59.22
FAKSA 42	96.01 ± 2.92	90.00 ± 1.32	40.03 ± 0.41	ND	ND	64.18 ± 0.81	235.18 ± 1.33	−37.45
FAKSA 43	39.27 ± 0.50	ND	226.10 ± 2.00	ND	138.00 ± 1.92	120.50 ± 1.36	305.79 ± 1.77	−77.93

* Antiviral activity of each extract expressed as normalized HCV copy numbers inhibition % after treating with each extract at 100 μg/mL, individually compared to control. Control cells = 100.

Tejedor et al. [41] reported that fungal tyrosinases not only showed high anti-HCV in Huh 5–2 hepatic cancer cells transfected with a replicon system and prevented the reproduction of the virus without prompting injuriousness in hepatic cells but also it demonstrated 10 times superior activity over the marketable drug ribavirin, so tyrosinases can be an innovative antiviral mechanism, through a conceivable catalytic mechanism of tyrosine residues in viral proteases.

Moreover, certain cancer cells are auxotrophic for methionine then deprivation of this amino acid by all fungal isolates in the current study could be a promising approach and source for targeting different kinds of cancer (Table 1). Isolates FAKSA 10, FAKSA 25, FAKSA 43, FAKSA 2 and FAKSA 34 gave the maximum methioninase yields, which was estimated at 242.70 ± 2.63, 226.10 ± 2.13, 226.10 ± 2.00, 213.36 ± 2.18 and 199.35 ± 1.88 U/gds, respectively (Table 1). In line with our results, Awad et al. [2] revealed that fungal L-methioninase selectively targeted and inhibited the proliferation of cancerous cells without damaging healthy cells because the deficiency of methionine synthase in malignant cells while healthy cells use it to make its needs of L-methionine. Among L-methionine sources, molds provide promising L-methioninase sources in various health concerns such as anti-oxidant, anti-cancer, anti-diabetes, anti-cardiovascular and against neurodegenerative diseases [42].

L-glutamine is deaminating to L-glutamic acid and ammonia by the action of the hydrolytic enzyme L-glutaminase. The capability of these isolates to produce the anticancerous L-glutaminase in Table 1 indicates FAKSA 10 as the best producer of L-glutaminase (235.30 ± 2.11 U/gds) followed by FAKSA 2, FAKSA 25, FAKSA 41, FAKSA 16, FAKSA-35 and FAKSA 1 (227.00 ± 2.18, 214.65 ± 1.95, 210.90 ± 2.12, 205.43 ± 2.09, 200.00 ± 2.05 and 190.34 ± 1.73 U/gds), respectively (Table 1). In the last decade, glutaminases had appealed considerable attention due to its widespread requests in medications as effective anti-leukemia and anti-retroviruses drug along with using as a flavor and aroma-enhancing agent in food industry [43].

Because L-asparaginase has powerful suppression activity against an extensive range of tumors, the current work investigates the productivity of this therapeutic enzyme from 43 marine endophytic fungi of soft coral (Table 1). The peak L-asparaginase secretion in descending order was achieved from endophytic fungi FAKSA 10 (180.20 ± 1.85 U/gds), FAKSA 25(171.68 ± 1.77 U/gds), FAKSA 38 (163.58 ± 1.71 U/gds), FAKSA 24 (160.27 ± 1.64 U/gds), FAKSA 2 (159.80 ± 1.83 U/gds), and FAKSA 6(156.30 ± 1.65 U/gds) (Table 1). El-Gendy et al. [9] obtained high amounts of L-asparaginases from *Fusarium equiseti* with hydrolyses and deprived properties toward the important nutrient for auxotrophic cancer cells, asparagine, and then, it caused starvation, apoptosis and proliferation inhibition for leukemic, cervix, liver, colon and breast carcinomas with IC_{50} ranged from 2.0 to 22.8 μg/mL.

Moreover, in ascending order, the overproducers for L-arginase were FAKSA 3 (105.13 ± 1.85 U/gds), FAKSA 15 (112.17 ± 1.95 U/gds), FAKSA 35 (119.65 ± 1.97 U/gds), FAKSA 25 (127.65 ± 1.97 U/gds), FAKSA 16 (133.20 ± 2.30 U/gds), FAKSA 43 (138.00 ± 1.92 U/gds), and FAKSA 10 (146.93 ± 2.00 U/gds) strains (Table 1). Li et al. [44] suggested that L-arginase (EC 3.5.3.1) which hydrolyzed L-arginine into L-ornithine and urea widely reported as an important anti-cancer mediator against auxotrophic cancers, particularly hepatocellular carcinoma and malignant melanoma in addition it works as antifungal, strengthening and protecting agents for the heart from endotoxin-induced shock.

As shown in Table 1, all endophytic isolates were able to produce noticeable amounts of ribonuclease (RNase). In particular, the highest RNase yields in descending order were recorded in the isolates FAKSA 10 (325.16 ± 1.90 U/gds), FAKSA 25 (319.20 ± 1 .85 U/gds), FAKSA 1 (317.32 ± 1.59 U/gds), FAKSA 13 (307.50 ± 1.57 U/gds), FAKSA 43 (305.79 ± 1.77U/gds), FAKSA 14 (296.32 ± 1.35 U/gds), FAKSA 6 (290.34 ± 1.25 U/gds), FAKSA 39 (284.20 ± 1.40 U/gds), FAKSA 16 (273.38 ± 1.65U/gds), FAKSA 30 (265.35 ± 1.69 U/gds) and FAKSA 18 (245.22 ± 1.55 U/gds), respectively (Table 1). These data indicated that the endophytic fungi under study have ribonucleolytic action toward viral genomes through catalyzing and degrading of viral RNA, which play roles in IFN stimulation, virus reproduction inhibition, and apoptosis induction as previously reported [10]. Moreover, the use of RNases in healing remains an attractive approach against several quite irredeemable tumors, such as mesothelioma or pancreatic malignance and against infectious diseases as well as against enveloped single-stranded RNA viruses was previously reported [11,45].

3.2. Screening of marine coral endophytic fungi for anti-HCV

Hepatitis C virus (HCV) currently infects more than 180 million people globally with annually 3 million newly infected people [3]. Data in Table 1 revealed that endophytic fungal microbiota of coral can be considered as a valuable source for antivirals targeting HCV with viral knockdown rate (VKR) ranging from −32.16% to −79.12%, (Table 1). Extract of endophytic fungi FAKSA 10 gave the maximum repression activity against HCV with VKR of −79.12% followed by FAKSA 43, FAKSA 16, FAKSA 25, FAKSA 35, FAKSA 3, FAKSA 6, FAKSA 15, FAKSA 14, FAKSA 23, FAKSA 40, FAKSA 2, and FAKSA 21 (VKR = −77.93, −75.92, −72.52, −71.00, 70.15, −69.20, −68.17, −66.85, −66.00, −65.96, −65.77, and −65.50%, respectively) (Table 1). A variety of fungal endophytes of corals and sponges including *Acremonium*, *Chaetomium*, *Aspergillus*, *Dothiorella*, *Lophiostoma*, *Fusarium*, *Penicillium* and *Trichoderma* species were reported as powerful HCV repressors [12]. From these findings in Table 1, we noticed that the hyperproducers of anti-HCV were the hyperactive producers of arginase, and thus, there is a correlation between the antiviral metabolites targeting HCV and the activity of arginase in fungi under study. These findings could be supported by Burrack and Morrison [46] as they suggested that arginine-hydrolyzing enzymes could limit the severity of viral pathogens comprising HIV, SARS, LCMV, HCV, RSV, and others due to myeloid cells impact the clearance of the viruses from host and the severity or resolution of tissue harm. Then among a total of 43 fungal isolates, the strain FAKSA10 that exhibited the maximum yields of pharmaceutical enzymes and anti-HCV activity using wheat bran as substrate in SSF was selected for further studies.

3.3. GC–MS analysis of the methanol extract of FAKSA 10 cultured on wheat bran medium

GC–MS analysis of crude extracts of strain FAKSA 10 demonstrated the existence of an extensive variety of bioactive products. Nine major compounds were detected in the chemical structure profile of the fungus FAKSA 10 with numerous bioactivities (Table 2, Fig. 2, and Fig. 3). For instant, 5α-Cholestane-3α, 25-diol (No. 13, RT 14.06, peak 0.68% has vital role in the therapy of metabolic disorders, hyperlipidemia and antioxidant activity); hexadecanoic acid, methyl ester (CAS) (No. 21, RT 32.0, 32.50% has anticancer, cytotoxic and antibacterial); hexadecanoic acid, ethyl ester (CAS) (No. 23, RT 33.20, 5.21% has antioxidant, hypocholesterolemic, anti-tumour, antibacterial and anti-androgenic activity); 9,12 octadecadienoic acid (Z, Z), methyl ester (CAS) (No. 25, RT 35.14, 25.52% has antiinfectious, antitumor, hepatoprotecting, anti-painful, anti-asthama and diuretic activity); 9-Octadecenoic acid (Z)-, methyl ester (CAS) (No. 26, RT 35.23, 11.37% with antimicrobial activity) (Table 2, Fig. 2, and Fig. 3). Moreover, heptacosanoic acid, methyl ester (CAS) (No. 27, RT 35.59, 1.53% with anticancer, cytotoxic and antibacterial); 11, 14-Eicosadienoic acid,

Table 2
GC–MS analysis of FAKSA 10 metabolites extracted from the wheat bran culture that showed a possible correlation with the observed biological activity.

No.	Compound name	RT (min)	Peak %	MW	Molecular formula	Biological activity
1	Methoxychromene precocene tetramer	5.47	0.70	760	$C_{48}H_{56}O_8$	Anti-juvenile
2	Methyl5amino6(7amino5,8 dihydro6methoxy5,8dioxo2quinolinyl) 4(3,4dimethoxy2(phenylmethoxy) phenyl3methyl2pyridinecarboxylate	6.24	0.48	610	$C_{33}H_{30}N_4O_8$	–
3	Cadmium chloride porphine derivative complex	6.99	0.43	607	$C_{29}H_{40}CdClN_5$	Therapy of colorectal cancer
4	5(Dibromomethyl)1,3bis(tribromomethyl)benzene	7.14	0.31	744	$C_9H_4Br_8$	Antimicrobial, antioxidant
5	[(Cyclopentadienyl)tris(diethylphosphitoP)cobaltO, O',O''] trichlorozirconium]	7.52	0.48	730	$C_{17}H_{35}C_{l3}CoO_9P_3Zr$	–
6	(7S,13E,16S,17R,18R, 19E,21R)7tertButyldimethylsilyloxy21hydr oxy17,18isopyopylide nedioxy16,18dimethy l10phenyl20phenylse leno[11]cytochalasa6(12),13,19trien1one	7.81	0.40	621	$C_{37}H_{55}NO_5Si$	–
7	N-Acetylaspartylglutamicacid	8.02	0.52	304	$C_{11}H_{16}N_2O_8$	Neuromodulator of glutamatergic synapses
8	2,7Bis[(2R,5R)2,5dih ydro2isopropyl3,6dim ethoxypyrazin5spiro) 1,2,3,6,7,8hexahydroasindacene	9.32	0.29	494	$C_{28}H_{38}N_4O_4$	–
9	21H,23HPorphine2,18dipropanoicacid,3,7,12,17tetramethyl8 ,13bis[2[(trimethylsilyl)oxy]ethyl], dimethyl ester (CAS)	9.69	0.29	770	$C_{42}H_{58}N_4O_6Si_2$	–
10	Methyl1-{4-Methoxy-3-chloro6-[2-[3(2′methoxy3′chloro5′(1,3-dioxan-2-yl) phenyl)-4-methoxyphenyl]ethyl]phenyl}-2-methoxybenzene-4-carboxylate	12.29	0.46	666	$C_{36}H_{36}C_{l2}O_8$	–
11	Tetraphenylporphyrinatodichlorotitanium(IV)	12.60	0.29	730	$C_{44}H_{28}C_{l2}N_4Ti$	Anticancer, antimicrobial
12	YGRKKRRQRRRGP VKRRLDL/5	12.78	0.35	2598	N/A	–
13	5 α –Cholestane-3 α, 25-diol	14.06	0.68	404	$C_{27}H_{48}O_2$	Treatment of metabolic syndromes, hyperlipidemia, diabetes, fatty liver and atherosclerosis
14	Dimethyl2anti-4anti-9,12anti-14-pentabromodecacyclo [9.9.0.0 (1,8).0(2,12). 0(6,10).0(11,18)0(13,17).0(16,20)]icosane-*syn*-4,*syn*-9-dicarboxylate	19.04	0.28	770	$C_{24}H_{23}Br_5O_4$	–
15	2,6,7-Tris-(2-methoxycarbonylethyl)-1,3,5,8-tetramethylporphin	20.23	0.44	624	$C_{36}H_{40}N_4O_6$	Photodynamic therapy of tumor
16	2-Decanol	22.60	0.35	158	$C_{10}H_{22}O$	Nematicide, neurotoxic
17	2,2′(Buta1,4-diyn-1,4-diyl) bis[(5,10,15,20-tetraphenylporphyrinato)zinc(II)]	23.53	0.35	1400	$C_{92}H_{56}N_8Zn_2$	–
18	Sulfurous acid,2-ethylhexyl hexyl ester	27.41	0.64	278	$C_{14}H_{30}O_3S$	–
19	YGRKKRRQRRRGP VKRRLFG/4	31.34	0.29	128	N/A	–
20	Hexane, 3-ethyl-3-methyl	31.73	0.56	128	C_9H_{20}	–
21	Hexadecanoic acid, methyl ester (CAS)	32.00	32.50	270	$C_{17}H_{34}O_2$	Anticancer, cytotoxic, antibacterial
22	1,2-Benzenedicarboxylic acid, butyl octyl ester (CAS)	32.69	0.31	334	$C_{20}H_{30}O_4$	–
23	Hexadecanoic acid, ethyl ester (CAS)	33.20	5.21	284	$C_{18}H_{36}O_2$	Antioxidant, hypocholesterolemic, antifungal, anti-tumour, antibacterial, anti-androgenic.
24	[(Phenyl)decasiloxane]	34.74	0.54	606	$C_6H_{14}O_{15}Si_{10}$	–
25	9,12Octadecadienoic acid (Z,Z), methyl ester (CAS)	35.14	25.52	294	$C_{19}H_{34}O_2$	Antimicrobial, anticancer, hepatoprotective, anti-arthritic, anti-asthama, diuretic
26	9-Octadecenoic acid(Z)-, methyl ester(CAS)	35.23	11.37	296	$C_{19}H_{36}O_2$	Antimicrobial
27	Heptacosanoic acid, methyl ester (CAS)	35.59	1.53	424	$C_{28}H_{56}O_2$	Anticancer, cytotoxic, antibacterial
28	11,14-Eicosadienoic acid, methyl ester	36.24	4.14	322	$C_{21}H_{38}O_2$	Antimicrobial, antioxidat activity
29	2,3Epoxypropylcycloheptane	36.32	1.33	154	$C_{10}H_{18}O$	Cytotoxic
30	13,14Dichlorobehenamide	36.77	0.89	407	$C_{22}H_{43}C_{l2}NO$	Carbonic anhydrase inhibitors, antiglaucoma
31	2(4)-(1-hydroxyethyl)-4(2)-(1-isopropoxyethyl) deuteroporphyrin dimethyl ether	38.02	0.42	668	$C_{39}H_{48}N_4O_6$	Catalysts, light sensitizers
32	9-Octadecenamide, (Z)-(CAS)	39.66	0.50	281	$C_{18}H_{35}NO$	–
33	2,5-Dibromo-1,4-di-n-hexadecylbenzene	44.04	0.48	682	$C_{38}H_{68}Br_2$	Cytotoxic
34	3-Bromo-N-(2′iodophenyl)2,5dimethoxybenzamide	44.29	0.33	460	$C_{15}H_{12}BrINO_3$	–
35	Dichloro(5,10,15,20tetraphenylporphyrinato)vanadium	47.50	0.44	733	$C_{44}H_{28}C_{l2}N_4V$	Antibacterial, anti-biofilm, cytotoxicity anticancer, antiviral, antioxidant and DNA protection activity
36	2-bis(ethoxycarbonyl)methyl-9(2,3,5-tri-O-(2-methylprop-2-yl) dimethyl silyloxy-α–D-ribofuranosyl)purine	47.91	0.56	752	$C_{35}H_{64}N_4O_8Si_3$	Antiviral
37	YGRKKRRQRRRGP VKRRLDL/5	48.17	0.31	2598	N/A	–
38	[(Cyclopentadienyl)tris(diethylphosphitoP)cobalt O, O',O''] trichlorozirconium	48.47	0.35	730	$C_{17}H_{35}C_{l3}CoO_9P_3Zr$	Antiviral, cytotoxic
39	Dimethyl2anti-4, anti-9,12, anti-14-pentabromodecacyclo [9.9.0.0 (1,8).0(2,12). 0(6,10).0(11,18)0(13,17).0(16,20)]icosanesyn-4, syn-9-dicarboxylate	48.86	0.34	770	$C_{24}H_{23}Br_5O_4$	–
40	2,2′,7,7′Tetrabromo9, 9′spirobifluorenone	49.76	0.47	628	$C_{25}H_{12}Br_4$	Strong oxidizing agents
41	Dodecachloroperylene	50.08	0.76	660	$C_{20}Cl_{12}$	–
42	CGNLSTCMLGTYTQ DLNKFHTFPQTSIGV GAP/2	50.38	0.35	3399	N/A	–
43	[2-(o-Methoxyphenyl)-5,10,15,20-tetraphenylporphyrinato] copper(II)	50.52	0.36	781	$C_{51}H_{34}CuN_4O$	–
44	4-Decyloxyphenyl3-ferrocenylbenzoate	52.82	0.29	538	$C_{33}H_{38}FeO_3$	Antifungal, antibacterial, Photo dynamic therapy

(*continued on next page*)

Table 2 (*continued*)

No.	Compound name	RT (min)	Peak %	MW	Molecular formula	Biological activity
45	(2Nitro5,10,15,20tet raphenyl[2(2)H1]prophyrinato)nickel(II)	53.77	0.30	715	$C_{44}H_{27}N_5NiO_2$	Antifungal, antibacterial
46	N,N'Bis[3methoxy4hydroxy5bromobenzylidene(cyano)acetyl]1, 4-butanediamine	54.19	0.36	646	$C_{26}H_{24}Br_2N_4O_6$	Anticancer, antiviral

RT: Retention time; MW: Molecular weight.

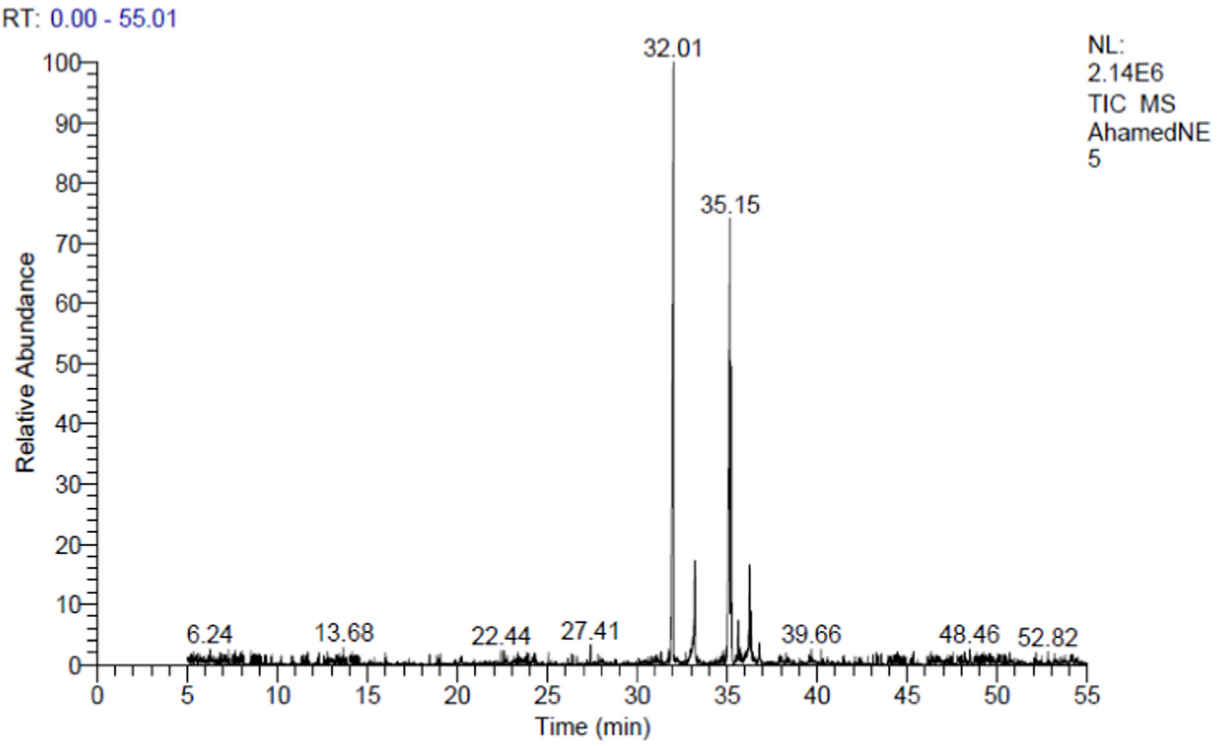

Fig. 2. GC–MS chromatograms of endophytic fungus strain FAKSA 10 derived extract from wheat bran culture.

methyl ester (No. 28, RT 36.24, 4.14% with antimicrobial and antioxidat activity); 2,3 epoxypropylcycloheptane (No.29, RT 36.32, 1.33% with cytotoxic activity) and 2-bis (ethoxycarbonyl) methyl-9 (2,3,5-tri-O-(2-methylprop-2-yl) dimethyl silyloxy-á-D-ribofuranosyl) purine (No. 36, RT 47.91, 0.52% with antiviral activity) were also detected in the extract of FAKSA 10. Many of these compounds have been previously reported as bioactive agents with several bioactivities containing antifungal, antibacterial, antidiabetic, antiviruses, antitumor, antioxidant, and anti-inflammation properties. For instance, tetraphenylporphyrinato dichlorotitanium (IV) acts as antibiotics, biosensors, tumor cell-killing and antimicrobial agents owing to its ability to form strong bonds with various biological molecules [47]. Furthermore, hexadecanoic acid, methyl ester (CAS) has antibacterial activity, Hexadecanoic acid, methyl ester and 9, 12-octadecadienoic acid methyl ester, (E, E)-(CAS) have been previously identified in the extract of *Aspergillus sydowii* with new antimalignance, cytotoxic, and antibacterial properties [48]. Furthermore, porphyrin/chlorin derivative as cadmium chloride porphine derivative complex is a promising molecule for colorectal cancer therapy [49], 5-cholesten, 3β-25-diol, disulfate used for healing metabolic syndromes, hyperlipidemia, diabetes and fatty liver [50].

However, lower peak areas $\leq$ 0.70% for several antiviral compounds including dichloro (5, 10, 15, 20 tetraphenylporphyrinato) vanadium (No. 35, RT 47.50, 0.44% with antiviral, antioxidant antibacterial, anti-biofilm, cytotoxicity, anticancer and DNA protection activity); [(cyclopentadienyl) tris (diethylphosphito P) cobalt O,O',O"]trichlorozirconium (No. 38, RT 48.47, 0.35% with antiviral activity and cytotoxic activity); and N, N'Bi [3–methoxy 4-hydroxyl 5-bromobenzylidene (cyano) acetyl] 1,4-butanediamine with antiviral and anticancer activity (No. 46, RT 54.19, 36% with antiviral activity and cytotoxic activity), N-Acetyl aspartyl glutamic acid (No. 7, RT = 8.02 min) as neuromodulator of glutamatergic synapses; methoxychromene precocene tetramer (No. 1, RT 5.47) as anti-juvenile; 2-decanol (No. 16, RT 22.60) as nematicide and neurotoxic and 13,14 dichlorobehenamide (No. 30, RT 36.77) as carbonic anhydrase inhibitor, an antiglaucoma and ophthalmology drug were detected in the extract of isolate FAKSA 10 (Table 2, Fig. 2, Fig. 3). Not only these compounds detected in the extract of FAKSA 10 but also other compounds such as 5 (dibromomethyl) 1,3 bis (tribromomethyl) benzene (No. 4, RT 7.14 with antimicrobial and antioxidant); tetraphenylporphyrinatodichlorotitanium (IV) (No. 11, RT 12.6 with antimicrobial and anticancer); 2, 6, 7-TRIS-(2-methoxycarbo

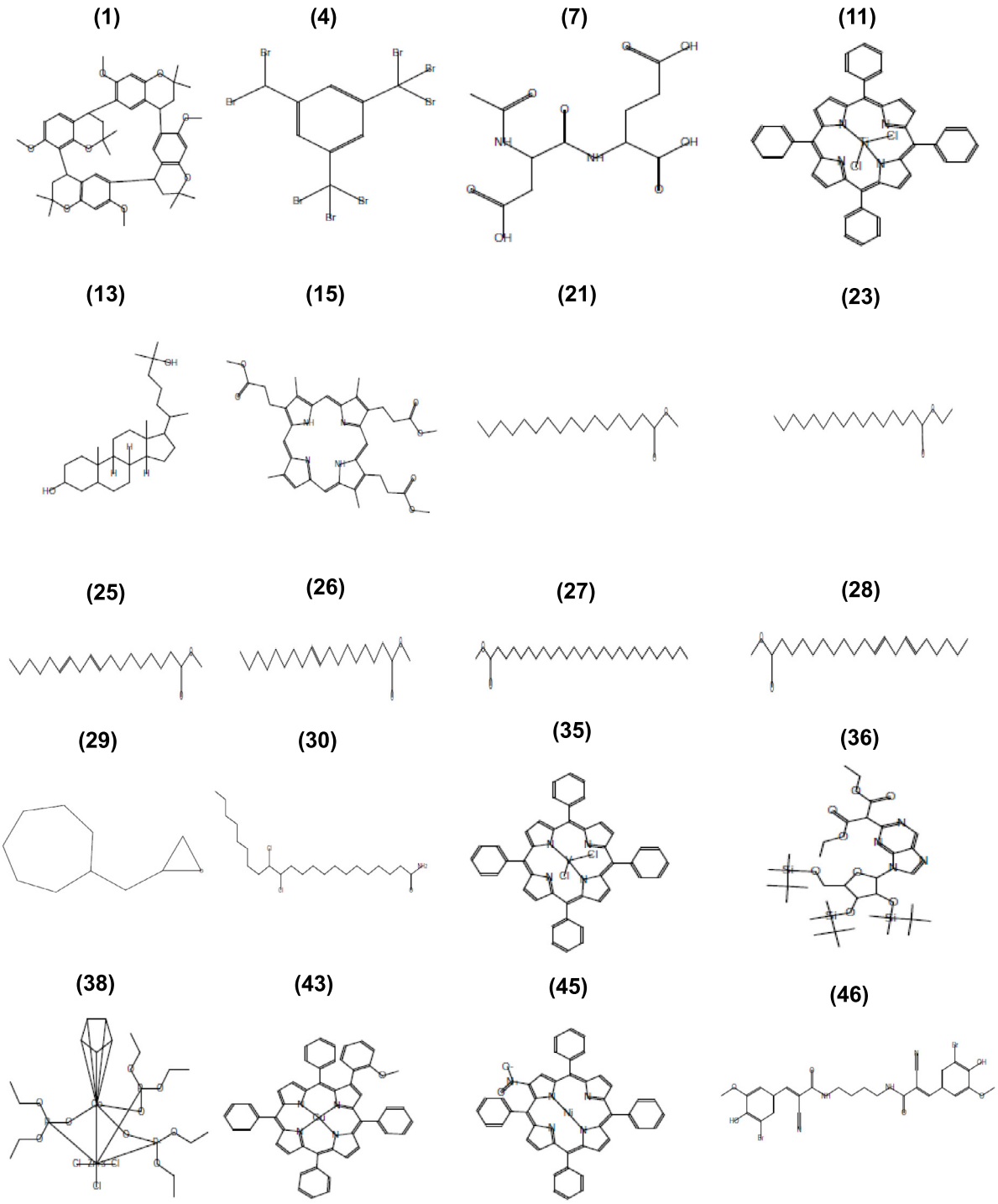

Fig. 3. Chemical structures of the identified metabolites that showed a possible correlation with the observed biological activity of endophytic fungus strain FAKSA 10 derived extract from wheat bran culture (the numbers mentioned are the numbers of these compounds in Table 2).

nylethyl)-1, 3, 5, 8-tetramethylporphin (No. 15, RT 20.23 with photodynamic therapy of tumor); [2-(o-Methoxyphenyl)-5,10,15,20-tetraphenylporphyrinato]copper (II) (No. 43, RT 50.52 with antifungal, antibacterial, and photo dynamic therapy) and (2 Nitro 5,10,15,20 tetraphenyl [2(2) H1] prophyrinato) nickel (II) (No. 45, RT 53.77 with antifungal, and antibacterial) were also detected in the extract of isolate FAKSA 10 on wheat bran medium (Table 2, Fig. 2, Fig. 3). The biological activities of these minor compounds have been previously reported by several authors [6,22,48,50,51].

3.4. Morphological, molecular and phylogeny study of the marine endophytic fungus FAKSA 10

Morphotypic description of the selected endophytic strain FAKSA 10 derived from the soft coral *S. polydactyla* in Table 3 and Figs. 4a,b,c was achieved on the basis of its micro- and macro-morphological features expressed. Strain FAKSA 10 showed a cylindrical, smooth, erect or flexuous, 36–88 µm long × 2.5–6.0 µm width conidiophore consisting of a smooth, dark brown, 2.5–

Table 3
Morphological characteristics of the selected fungal strain FAKSA 10.

Morphological character	Description
Conidiophores	Cylindrical, basauxic, smooth, erect or flexuous, thick and multieseptate, 36–88 μm long × 2.5–6.0 μm width containing flat branched hyphae, 2.5–6.0 μm in diam and septate with dark brown septa.
Conidiogenous cells	Basauxic, 4.5–9 × 2–5 μm, arise from conidiophore mother cell, erect, ampulliform or doliiform, pale brown.
Conidiophore mother cells	Short, thick, formed by superficial mycelium, emerging in clusters or solitary, 4–9 × 4–8 μm, colorless except for brown or dark brown transverse septa, ampulliform to lageniform.
Conidia	Borne in grape-like bunch, dark brownish, smooth-walled and aseptate, globose to lenticular in shape with dark germ slit, measuring 8–10 μm long in face view, 4.5–6.5 μm in side view.
Sterile cells	Terminal or subterminal, having solitary or more cubic bodies, globose to ellipsoid, very pale brown, smaller and lighter than conidia.
PDA*	Colonies 65 mm, thick, compact, round, entire margin, wooly, concentrically spreading with aerial mycelium, surface view of culture is white turned to whitish gray and reverse yellowish; dark olive-brown diffused pigment.
MEA*	Colonies creamy white, reverse pale yellow, circular, 70 mm diam, smooth, sparse aerial mycelium, circular edge; neither sporulation nor pigment produced.
OA*	Colonies 60 mm, abundant, concentrically spreading with aerial mycelium, spherical border; mycelia whitish to pinkish; sporulation was not detected; pink diffused pigment noticed.

* Culture characteristics after 14 d.

6.0 μm in diam and septate hyphae with dark brown septa. Basauxic conidiogenous cell arise from conidiophore mother cell, 4.5–9 × 2–5 μm, erect, sub-globose, smooth and hyaline to brown. Conidiophore mother cells were short, thick, formed by superficial mycelium, emerging in clusters on hyphae or solitary, 4–9 × 4–8 μm, colorless except for brown or dark brown transverse septa. Conidia born in grape-like bunch, dark brownish, smooth-walled and aseptate, globose to lenticular in shape with dark germ slit measuring 8–10 μm long in face view and 4.5–6.5 μm in side view. The sterile cells were terminal or subterminal, had solitary or more cubic bodies, and were globose to ellipsoid, very pale brown, smaller and lighter than conidia. Pintos et al. [17] stated that *Arthrinium* has varied morphological characteristics than other anamorphic types of xylariaceous such as the existence of basauxic conidiogenous cell arised from conidiophore mother cell and dark, aseptate conidia with a hyaline edge. Moreover, cultures of strain FAKSA 10 on PDA were 65 mm, thick, compact, round, concentrically dispersal with aerial mycelia, entire margin, wooly, white turned to whitish grey, reverse yellowish, dark olive-brown diffused were produced (Table 3). Malt extract agar cultures showed creamy white, reverse pale yellow, circular, flat colonies, 70 mm diam, concentrically dispersal, and rounded margin. OA cultures showed white to pink, colonies of 60 mm, thick, concentrically dispersal with aerial mycelia, spherical edge; pinkish diffused pigment (Table 3). Therefore, based on morphological criteria, the selected endophytic fungal isolate FAKSA 10 was obtained from marine soft coral *S. polydactyla* belonged to *Arthrinium* sp. (Table 3 and Figs. 4a,b,c). *Arthrinium* species have traditionally been classified based on morphological characteristics such as conidial shape, conidiophores, the presence or absence of sterile cells and the other taxonomical properties as previously described [17,28,29,30,31].

The classification according to the ITS region of strain FAKSA 10 was conducted to confirm the phenotypic characterization and to define the phylogeny relations between the taxa, and to resolute closely correlated species. The amplification of the ITS1-5.8S-ITS2 region of rDNA for the selected marine endophyte strain FAKSA 10 by means of the widespread primers ITS1 and ITS4 originated a fragment of approximately 566 bp. The sequence of the ITS region of the selected strain FAKSA 10 was amplified, sequenced and submitted to GenBank under accession number (PP891624). A BLAST analysis done through blastn search through GenBank exhibited that FAKSA 10 fungus belongs to *Ascomycota* and genus *Arthrinium*. As shown in Fig. 5, isolate FAKSA 10 fitted well with the genus *Arthrinium* and it clustered with *Arthrinium* sp. MUT 1745, Po15, and CUZF35HIK (99.61, 98.59, and 98.50%), respectively, as well as the selected isolate showed a similarity of 98.93, and 98.39% with *Arthrinium arundinis*, and *Arthrinium phaeospermum* Po17, respectively. Consequently, depending on phenotypic and sequence data, the selected endophytic fungal isolate FAKSA 10 attained from coral *S. polydactyla* identified and designated as *Arthrinium* sp. FAKSA 10 (Table 3, Figs. 4a,b,c, Fig. 5). Phylogeny study is the key procedure in the actuality of the taxonomy of fungi [33]. Currently, 80 species of *Arthrinium* have been described in catalog Fungorum; however, maximum of the *Arthri-*

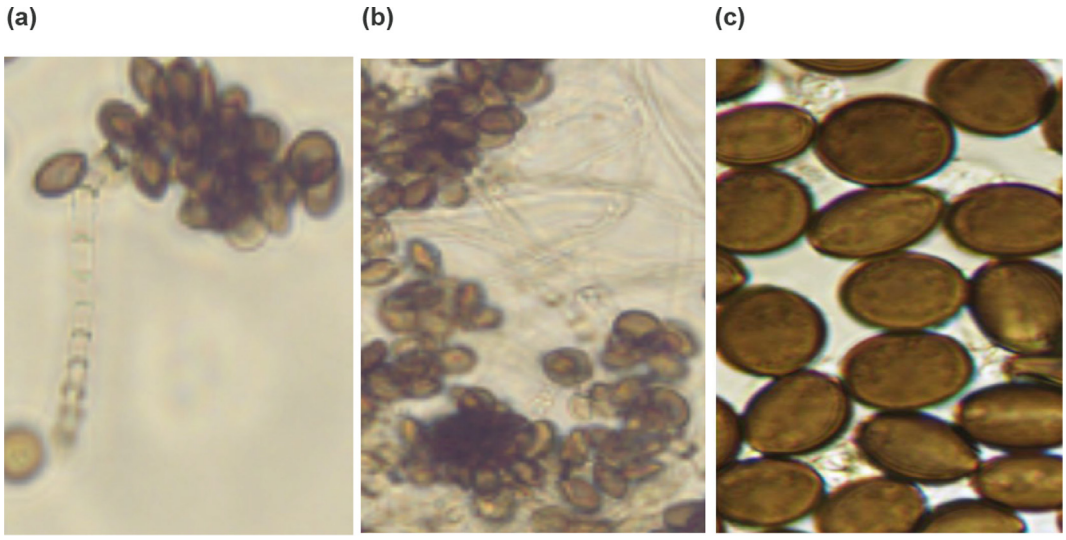

Fig. 4. Morphological characteristics of the selected fungal strain FAKSA 10. Conidia, conidiogenous cells, and hyaline conidiophores with brown septa (a, b) and conidia (c). Scale bars: (a, b) = 200 μm, (c) = 5 μm.

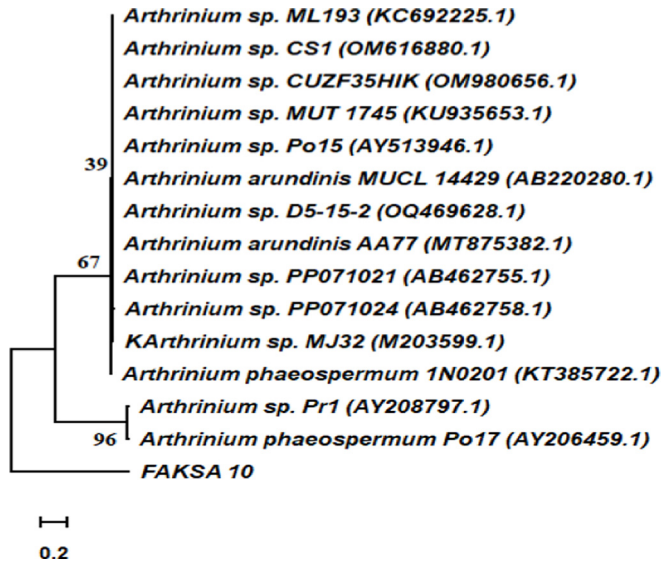

Fig. 5. Phylogenetic tree of selected marine endophytic fungus *Arthrinium* sp. FAKSA 10 of soft coral constructed by neighbor-joining method based on rDNA-ITS sequences.

nium taxa have no sufficient sequence results and absence of a complete characterization of their phenotypic characters [31,52]. Furthermore, Heo et al. [22] reported that 28 marine endophytic *Arthrinium* strains were identified using phylogenetic analysis followed by building a phylogenetic tree by pooled data from ITS and then classified into fifteen species, comprising eleven new species.

3.5. Optimization of SSF systems for the selected endophytic fungus *Arthrinium sp. FAKSA 10*

Choosing the substrate and optimizing the growth conditions are critical to constructing an efficient SSF system to accelerate the production of bioactive metabolites. Then, 11 agro-industrial wastes including brans of wheat and rice; oil cakes of palm, olive, wheat, sesame, almond, mustard and coconut; and peels of pomegranate and banana sized to 2 mm with initial moisture content of 60% were evaluated, individually as production media for varied bioactive metabolites by endophytic *Arthrinium* sp. FAKSA 10 under SSF at 28°C for 14 d (Table 4, Table 5). After that, the other parameters of SSF including incubation period, particle size, initial moisture content, incubation temperature, and inoculum size were also optimized.

3.5.1. Screening of solid substrates as production medium for different biologically active agents

3.5.1.1. Pharmaceutical enzymes. To determine the appropriate components in the medium for enzyme production, the impact of 11 solid wastes as low-cost production media was evaluated. The data in Table 4 revealed that the oil cakes of palm (174.38 ± 2.30 U/gds, respectively) followed by mustard (160.71 ± 2.05 U/gds), olive (145.53 ± 2.19 U/gds) and coconut (126.95 ± 1.40 U/gds) were the best inducer for the highest biosynthesis of L-lysine α-oxidase compared to 132.53 ± 2.01 U/gds produced on wheat bran culture. Our results are in agreement with Costa et al. [7], as they reported that among 11 agro-industrial by-products, substrates under SSF rice bran followed by wheat bran and cotton seed cake were the optimum solid substrate for the induction of enzyme from *Trichoderma harzianum*.

Appreciate amounts of L-glutaminase and L-arginase were detected in all agro-industrial residues used as cultivation media but maximum yields were noticed in medium composed of palm (398.52 ± 2.95 and 190.37 ± 2.86 U/gds), mustard (357.01 ± 2.69 and 175.43 ± 2.70 U/gds), olive (340.51 ± 2.74 and 163.02 ± 2.42 U/gds), coconut (306.62 ± 2.00 and 160.25 ± 2.34 U/gds), and almond (290.74 ± 2.14 and 150.12 ± 2.27 U/gds) oil cakes, separately (Table 4).

As shown in Table 4, mustard oil cake medium was the most proper for producing L-tyrosinase, L-methioninase, and L-asparaginase by giving maximum yields (140.34 ± 1.45, 295.30 ± 2 .42 and 230.44 ± 2.57 U/gds) of enzymes followed by palm oil cake (120.15 ± 1.41, 280.40 ± 2.58 and 214.25 ± 2.21 U/gds), olive oil cake (119.62 ± 1.37, 254.92 ± 2.51 and 196.90 ± 1.68 U/gds), wheat bran (97.12 ± 1.19, 242.70 ± 2.63 and 180.20 ± 1.85 U/gds), and coconut oil cake (95.40 ± 0.82, 220.50 ± 2.10 and 173.00 ± 1.05 U/gds), respectively (Table 4). In accordance with the current work, Swathi and Dhanalakshmi [18] screened various by-products for producing methioninase from *Aspergillus flavipes* 8, such as oil cakes of sesame, coconut, soya bean, palm, neem and groundnut as well as orange peel, tea waste, and among them, sesame oil cake gave the highest yield (208 U/gds). Among various agro-industrial materials, peel of pomegranate, potato and orange were reported to be the fit carbon sources for the maximal formation of L-glutaminase (160.3, 59.2 and 35.6 U/gds) from Fusarium solani while pomegranate peel was selected as the best carbon source among others to give the maximum yields of L-asparaginase from *Fusarium oxysporum* F-S3 under solid state fermentation [20,43].

Data presented in Table 4 shown that oil cakes of palm (POC), mustard (MOC) and olive (OOC) share positive stimulatory effects on the strain to produce all the pharmaceutical enzymes under study and subsequently, these substrates were combined in different ratios (1:1:1, 2:1:1, 1:2:1, and 1:1:2) to formulate the best production medium for these bioactive metabolites. Interestingly, the medium composed of POC + MOC + OOC at a ratio of 2:1:1 increased L-lysine α-oxidase, L-arginase, and L-glutaminase by 1.58-, 1.60- and 1.22-fold, respectively, compared to the best inducer POC alone (Table 4). On the other hand, a fermentation medium composed of POC + MOC + OOC at a concentration of 1:2:1 improved the productivity of L-tyrosinase, L-methioninase, and L-asparaginase by the selected fungus strain *Arthrinium* sp. FAKSA 10 by 61.41, 41.74, and 57.39%, respectively, compared to the MOC medium (Table 4). Then, in the current work, a mixture of POC + MOC + OOC at a concentration of 2:1:1 was used and recommended as the production medium for the pharmaceutical enzymes L-lysine α-oxidase, L-arginase and L-glutaminase while these solid substrates at concentration of 1:2:1 recommended for the best production of L-tyrosinase, L-methioninase, and L-asparaginase without any supplementations.

RNase activity varied with changing solid substrates used. In escalating order, they were pomegranate peel, almond oil cake, coconut oil cake, rice bran, banana peel, wheat germ oil cake, wheat bran, sesame oil cake, mustard oil cake, palm oil cake, and olive oil cake (200.83 ± 1.60, 252.50 ± 1.89, 256.00 ± 1.72, 300.62 ± 1.89, 309.40 ± 1.94, 312.26 ± 1.90, 325.16 ± 2.07, 340.21 ± 2.08, 350.12 ± 2.40, 351.74 ± 2.20, and 368.06 ± 2.33 U/gds) (Table 4). Then, compared to the wheat bran medium (WB), the production medium composed of olive, palm and mustard oil cakes, individually, has a tendency to increase RNase production from strain FAKSA 10 by 1.13-, 1.08-, and 1.08-fold as a control. These best inducers were combined at different ratios to identify suitable fermentative substrates for RNase activity. Data in Table 4 proved that using a medium composed of POC + MOC + OOC mixture at a ratio of 1:1:2 maintained the maximum RNase production, which increased by 28.84, 34.81 and 35.44% compared to oil cake of olive, palm or mustard, respectively, as fermentative substrate alone by strain FAKSA 10 (Table 4).

3.5.1.2. Anti-Hepatitus C virus (anti-HCV). Anti-HCV activity expressed as IC_{50} values was detected in all fermented substrates with peaks in the oil cakes of olive (14.90 ± 0.98 μg/mL), mustard

Table 4
Effect of different agro-industrial residues as substrates on the production of pharmaceutical enzymes by *Arthrinium* sp. FAKSA 10 under solid-state fermentation.

Solid substrate	Pharmaceutical enzymes (U/gds)						
	L-Lysine α-Oxidase	L-Tyrosinase	L-Methioninase	L-Asparaginase	L-Arginase	L-Glutaminase	RNase
Wheat bran (WB, Control)	132.53 ± 2.01	97.12 ± 1.19	242.70 ± 2.63	180.20 ± 1.85	146.93 ± 2.00	235.30 ± 2.11	325.16 ± 2.07
Palm oil cake (POC)	174.38 ± 2.30	120.15 ± 1.41	280.40 ± 2.58	214.25 ± 2.21	190.37 ± 2.86	398.52 ± 2.95	351.74 ± 2.20
Olive oil cake (OOC)	145.53 ± 2.19	119.62 ± 1.37	254.92 ± 2.51	196.90 ± 1.68	163.02 ± 2.42	340.51 ± 2.74	368.06 ± 2.33
Wheat germ oil cake (WGC)	119.45 ± 1.86	85.25 ± 1.06	195.90 ± 2.18	143.90 ± 1.53	128.16 ± 1.85	230.57 ± 2.20	312.26 ± 1.90
Sesame oil cake (SOC)	116.90 ± 1.80	90.80 ± 1.17	131.28 ± 1.91	137.94 ± 1.60	107.49 ± 1.67	214.65 ± 1.95	340.21 ± 2.08
Almond oil cake (AOC)	100.00 ± 1.72	86.28 ± 1.17	200.44 ± 2.13	163.50 ± 1.79	150.12 ± 2.27	290.74 ± 2.14	252.50 ± 1.89
Mustard oil cake (MOC)	160.71 ± 2.05	140.34 ± 1.45	295.30 ± 2.42	230.44 ± 2.57	175.43 ± 2.70	357.01 ± 2.69	350.12 ± 2.40
Coconut oil cake (COC)	126.95 ± 1.40	95.40 ± 0.82	220.50 ± 2.10	173.00 ± 1.05	160.25 ± 2.34	306.62 ± 2.00	256.00 ± 1.72
Pomegranate peel (POP)	95.30 ± 2.13	67.23 ± 1.11	201.90 ± 1.50	91.18 ± 1.30	133.40 ± 1.94	239.92 ± 1.25	200.83 ± 1.60
Banana peel (BP)	84.79 ± 1.54	89.65 ± 1.00	117.86 ± 2.33	68.24 ± 0.99	140.20 ± 1.99	148.50 ± 1.93	309.40 ± 1.94
Rice bran (RB)	119.28 ± 2.01	92.50 ± 1.16	220.18 ± 2.53	137.90 ± 1.64	130.57 ± 1.90	265.70 ± 2.29	300.62 ± 1.89
POC + MOC + OOC (1:1:1)	230.37 ± 2.50	165.20 ± 1.62	339.13 ± 2.90	272.03 ± 2.69	248.03 ± 3.50	428.03 ± 3.15	442.38 ± 3.18
POC + MOC + OOC (2:1:1)	276.29 ± 2.47	209.03 ± 1.85	375.20 ± 3.15	318.42 ± 2.85	304.92 ± 3.94	486.50 ± 3.43	430.27 ± 3.06
POC + MOC + OOC (1:2:1)	249.55 ± 2.32	226.52 ± 1.95	418.55 ± 3.28	362.71 ± 2.98	280.55 ± 3.76	450.55 ± 3.36	434.00 ± 3.28
POC + MOC + OOC (1:1:2)	231.48 ± 2.25	188.36 ± 1.75	342.55 ± 2.96	296.42 ± 2.60	250.55 ± 3.52	439.55 ± 3.28	474.19 ± 3.28

Table 5
Optimization of solid-state fermentation process parameter on the anti-HCV, antioxidant and anticancer activities by *Arthrinium* sp. FAKSA 10.

Solid substrates	Anti-hepatitis C virus (IC_{50}; μg/mL)	Antioxidant potential		Anti-proliferative activity (IC_{50}; μg/mL)		
		DPPH scavenging activity (IC_{50} μg/mL)	Reducing power assay	Cancerous cells		Normal cells
				HepG-2	HCT-116	WI-38
Wheat bran (Control)	59.00 ± 2.23	80.11 ± 0.99	0.514	39.43 ± 2.18	34.40 ± 2.13	400.28 ± 10.47
Palm oil cake (POC)	22.61 ± 1.48	33.23 ± 0.09	0.866	20.69 ± 1.42	20.47 ± 1.52	350.19 ± 9.88
Olive oil cake (OOC)	14.90 ± 0.98	28.19 ± 1.09	0.884	16.80 ± 1.23	18.00 ± 1.36	310.34 ± 9.70
Wheat germ oil cake (WGC)	37.29 ± 1.76	76.84 ± 1.92	0.540	30.16 ± 2.05	33.62 ± 2.19	425.00 ± 11.18
Sesame oil cake (SOC)	16.34 ± 1.13	19.59 ± 0.98	0.951	15.12 ± 1.19	13.47 ± 1.14	390.27 ± 10.58
Almond oil cake (AOC)	20.18 ± 1.40	16.71 ± 0.33	0.974	18.38 ± 1.35	19.47 ± 1.50	367.91 ± 9.76
Coconut oil cake (COC)	26.58 ± 1.65	30.36 ± 0.46	0.879	24.39 ± 1.71	20.56 ± 1.59	395.84 ± 10.47
Mustard oil cake (MOC)	15.67 ± 1.29	24.12 ± 0.25	0.895	12.62 ± 1.13	15.60 ± 1.28	380.56 ± 9.91
Pomegranate peel (POP)	40.26 ± 1.88	50.28 ± 0.37	0.692	20.48 ± 1.50	20.63 ± 1.53	276.55 ± 8.95
Banana peel (BP)	60.15 ± 2.28	71.04 ± 0.49	0.560	37.05 ± 2.17	31.25 ± 2.11	390.13 ± 10.55
Rice bran (RB)	57.20 ± 2.15	75.90 ± 0.50	0.539	39.70 ± 2.14	37.49 ± 2.20	415.85 ± 11.29
OOC + SOC + AOC + MOC (1:1:1:1)	18.24 ± 0.98	15.30 ± 1.38	0.980	15.37 ± 1.14	15.00 ± 1.21	321.00 ± 8.95
OOC + SOC + AOC + MOC (2:1:1:1)	11.22 ± 1.03	15.01 ± 1.37	0.984	13.95 ± 1.22	16.75 ± 1.27	340.65 ± 9.38
OOC + SOC + AOC + MOC (1:2:1:1)	15.18 ± 1.16	12.50 ± 1.24	0.990	12.56 ± 1.16	11.22 ± 1.00	359.73 ± 9.70
OOC + SOC + AOC + MOC (1:1:2:1)	18.56 ± 1.02	11.80 ± 1.19	0.998	17.20 ± 1.30	15.90 ± 1.31	307.15 ± 8.29
OOC + SOC + AOC + MOC (1:1:1:2)	13.20 ± 0.81	14.25 ± 1.45	0.990	10.30 ± 1.04	11.00 ± 1.15	396.80 ± 10.50
Telaprevir	41.53 ± 2.00	ND	ND	ND	ND	ND
Ascorbic acid	ND	34.26 ± 1. 28	0.988	ND	ND	ND
Doxorubicin (Doxo)	ND	ND	ND	4.20 ± 0.27	5.12 ± 0.32	54.69 ± 3.18

(15.67 ± 1.29 μg/mL), sesame (16.34 ± 1.13 μg/mL), almond (20.1 8 ± 1.40 μg/mL), palm (22.61 ± 1.48 μg/mL), coconut (26.58 ± 1.6 5 μg/mL) and wheat germ (37.29 ± 1.76 μg/mL); pomegranate peel (40.26 ± 1.88 μg/mL); brans of rice (57.2 ± 2.15 μg/mL) and wheat (59.00 ± 2.23 μg/mL); and banana peel (60.15 ± 2.28 μg/mL), respectively (Table 5). The highest inhibition of HCV replication with the lowest IC_{50} on these substrates can be attributed to these substrates are inducers for the production of tyrosinase, arginase, RNase and L-lysine α-oxidase which are involved in anti-HCV activity in fungi and actinomycetes. Therefore, a medium composed of olive, sesame, almond and mustard oil cakes at different ratios was tested to identify suitable fermentative medium for antiviral metabolites production. As shown in Table 5, the fermentation medium composed of OOC, SOC, AOC, and MOC (2:1:1:1) increased the viral inhibition at lower IC_{50} 11.22 ± 1.03 μg/mL than each individual substrate. The formulated medium not only increased the anti-HCV activity but also increased all pharmaceutical enzymes that could be targeting HCV. In similar, Lopez-Tejedor et al. [41] stated that tyrosinases from *Agaricus bisporus* extract showed high cell toxicity and antiviral activity against hepatitis C virus replication with no prompting toxicity in hepatic cells with ten times higher than the marketable medication ribavirin. Then, the current work represents antiviral inhibition approaches depending on the amino acid-depleting enzymes, which are produced under low-cost procedures. The powerful action of these enzymes in the current work to viral pathogens could be attributed to their catalytic activity toward certain amino acid residues in proteases of varied ranges of viruses [3].

3.5.1.3. Antioxidant properties. High DPPH radical-scavenging activity and reducing power antioxidant associated with lower IC_{50} and higher values at OD_{700} nm, respectively, were obtained in ascending order from the fermented substrates of pomegranate peel (IC_{50} = 50.28 ± 0.37 μg/mL, OD_{700} = 0.692), palm cake (IC_{50} = 33.2 3 ± 0.09 μg/mL, OD_{700} = 0.866), coconut cake (IC_{50} = 30.36 ± 0.46 μg/mL, OD_{700} = 0.879), olive cake (IC_{50} = 28.19 ± 1.09 μg/mL, OD_{700} = 0.884), mustard cake (IC_{50} = 24.12 ± 0.25 μg/mL, OD_{700} = 0.895), sesame cake (IC_{50} = 19.59 ± 0.98 μg/mL,

OD_{700} = 0.951), and almond cake (IC_{50} = 16.71 ± 0.33 μg/mL, OD_{700} = 0.974) by *Arthrinium* sp. FAKSA 10 (Table 5). However, the lowest antioxidant activity was achieved from the fermented substrates of wheat bran (IC_{50} = 80.11 ± 0.99 μg/mL, OD_{700} = 0.514), wheat germ oil cake (IC_{50} = 76.84 ± 1.92 μg/mL, OD_{700} = 0.540), rice bran (IC_{50} = 75.90 ± 0.50 μg/mL, OD_{700} = 0.539), and banana peel (IC_{50} = 71.04 ± 0.49 μg/mL, OD_{700} = 0.560), respectively (Table 5). Reactive oxygen species (ROS) were accountable for various types of health problems and aging through damaging diverse biological molecules like DNA, protein and lipids by oxidating cellular reactions [6]. Marine algicolous *Arthrinium* species are sources of a varied array of potent natural products with radical-scavenging capabilities that could scavenge-free radicals produced from ROS [22]. As shown in Table 5, when the fermentation medium is composed of a mixture of OOC, SOC, AOC, and MOC at a concentration of 1:1:2:1, the highest DPPH radical-scavenging ability through decreasing IC_{50} to 11.80 ± 1.19 μg/mL was achieved as well as reducing power activity increased at OD_{700} to 0.998. In agreement with our results, Heo et al. [22] recommended marine *Arthrinium* species such as *A. sacchari* KUC21340, *A. saccharicola* KUC21221, *A. saccharicola* KUC21343, and *Arthrinium* sp. KUC21332 are a huge source of natural antioxidants against the 2,2-diphenyl-1-picrylhydrazyl (DPPH) radical. This proposed that the endophytism correlation between *Arthrinium* species and their hosts of coral or sponge in marine might stand on regulating of ROS-defense system owing to their abundant antioxidant capability as previously reported [53].

3.5.1.4. Anticancer activity. In this study, the anti-proliferative activity of the fungus *Arthrinium* sp. FAKSA 10 extracts after growing on different agroindustrial residues was evaluated against liver (HepG-2) and colon (HCT-116) carcinoma cells along with normal lung fibroblasts (WI-38) cells. The IC_{50} values of FAKSA 10 extracts against cancer cells were considerably lower than those of normal cells. In descending order, the best oil cake-based medium with the lowest IC_{50} toward HepG-2 cells was mustard oil cakes (12.62 ± 1.13), sesame oil cake (15.12 ± 1.19) and olive oil cake (16.80 ± 1.23) (Table 5). Oil cake cultures of sesame and mustard gave the lowest IC_{50} of 13.47 ± 1.14 and 15.60 ± 1.28 μg/mL, respectively, against HCT-116 cells (Table 5). Likewise, endophytic *A. arundinis* in solid medium gave twelve cytochalasans and arundisins compound, out of them arundisins A and B displayed cytotoxicity against breast carcinoma cells with IC_{50} = 18.82 and 15.20 μM [54]. In contrast, the fungus FAKSA 10 failed to induce cytotoxicity in normal cells WI-38 at a concentration that was cytotoxic to cancer cells. The IC_{50} values of all extracts derived from FAKSA 10 fungus cultured on all agroindustrial residues-based media were significantly higher ≥ 276.55 ± 8.95 to ≤ 425.00 ± 11.18 μg/mL (Table 5). Then, FAKSA 10 extracts derived from low-cost production media have a highly desirable selectivity trait toward cancer cells for a potential therapeutic anti-cancer agent (Table 5). Compared to control cells, FAKSA 10 extract showed cytotoxic effects and alterations in the morphology of cell lines in a dose-dependent manner (Fig. 6a–h). These changes in both carcinoma cells included monolayer disruption; accumulation in polygonal cells as they shrink, took sphere-shaped and / or lysed after 2 d' treatment (Fig. 6a–h).

Moreover, compared to the individual substrates, the medium composed of OOC, SOC, AOC, and MOC mixture at 1:1:1:2 reduced the IC_{50} of FAKSA 10 extract to 10.30 ± 1.04 μg/mL against HepG-2 and 11.00 ± 1.15 μg/mL toward HCT-116 cells (Table 5). Consistent with our findings, *Arthrinium* species of marine sponge gave biologically active products with antiproliferative (arthrinins A-D), antiangiogenic (decarboxyhydroxycitrinone, myrocin A, libertellenone C, and cytochalasin E) and cytotoxic (cytochalasin K and 10-phenyl-[12]-cytochalasin Z16) activities [31,55]. Furthermore, different bioactive cytochalasans were isolated from the fungus *A. arundinis* DJ-13 with different antioxidant and anticancer activity [54].

3.5.2. Optimization of the SSF factors for the production of bioactive metabolites by Arthrinium sp. FAKSA 10

Among the different incubation periods ranging from 5 to 20 d, 10 d supported the highest production of L-methioninase, L-lysine α-oxidase, L-tyrosinase, L-asparaginase, L-arginase, L-glutaminase and RNase (417.90 ± 3.30, 275.29 ± 2.43, 226.52 ± 1.95, 360.88 ± 2.94, 305.00 ± 3.60, 486.38 ± 3.40, and 474.28 ± 3.25 U/gds) were achieved (Table 6). At lower or higher incubation periods, the productivity of these enzymes decreased. The particle size of any substrate used in SSF has a prominent impact on microbial growth and enzyme production [43]. By reducing the particle size of the substrates used in SSF from 2 mm to 1.0 mm, there were increases in L-lysineα-oxidase from 276.29 ± 2.47 to 328.40 ± 2.80 U/gds, L-tyrosinase from 226.52 ± 1.94 to 294.18 ± 2.15 U/gds, L-methioninase from 417.23 ± 3.31 to 500.46 ± 3.73 U/gds, L-asparaginase from 360.88 ± 2.94 to 458.65 ± 2.86 U/gds, L-arginase from 305.00 ± 3.60 to 422.03 ± 3.85 U/gds, L-glutaminase from 487.16 ± 3.50 to 511.20 ± 3.90 U/gds and RNase from 475.12 ± 3.31 to 545.23 ± 3.55 U/gds (Table 6). The L-methioninase, L-lysine α-oxidase, L-tyrosinase, L-asparaginase, L-

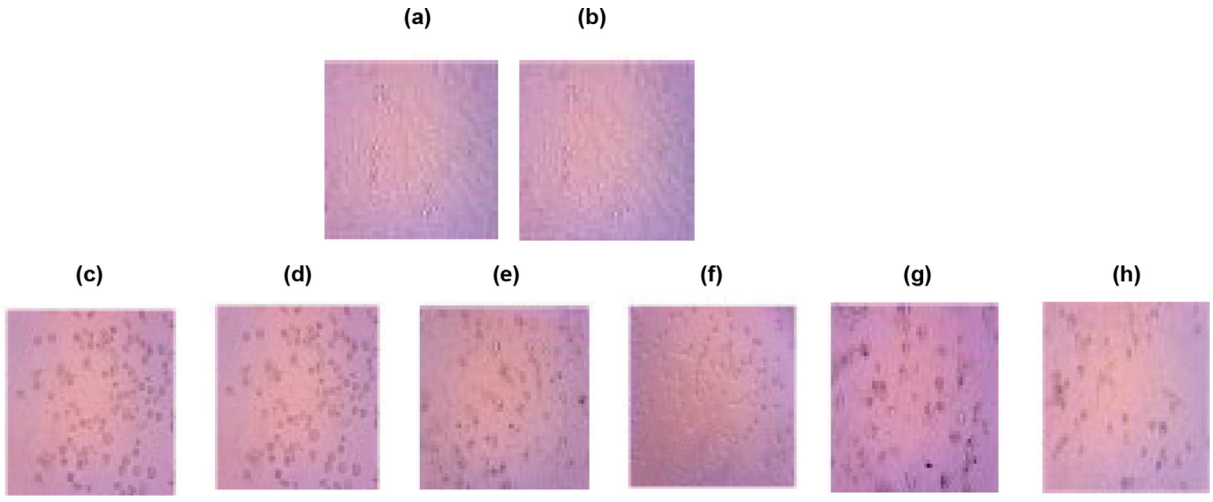

Fig. 6. Morphological changes of HepG-2 and HCT-116 monolayers. Control HepG-2 (a) and HCT-116 (b) cells (treated with 0.5% DMSO). Treated cells HepG-2 (c, e and g) and HCT-116 (d, f and h) treated with 5.0, 10 and 25 μg/mL of extract. Total magnification = × 100.

Table 6
Optimization of SSF process parameters for the productivity of pharmaceutical enzymes by *Arthrinium* sp. FAKSA 10.

Process parameter	Amino acid degrading enzyme production (U/gds)						
	L-Lysine α-Oxidase	L-Tyrosinase	L-Methioninase	L-Asparaginase	L-Arginase	L-Glutaminase	RNase
Incubation period (d)							
5	128.54 ± 2.19	108.88 ± 1.32	196.30 ± 2.71	218.50 ± 2.28	162.14 ± 2.75	304.91 ± 2.45	202.85 ± 1.92
7	194.38 ± 2.25	127.13 ± 1.50	320.55 ± 3.14	280.36 ± 2.50	235.20 ± 3.28	390.45 ± 2.96	300.42 ± 2.38
10 (control)	275.29 ± 2.43	226.52 ± 1.95	417.90 ± 3.30	360.88 ± 2.94	305.00 ± 3.60	486.38 ± 3.40	474.28 ± 3.25
14	225.20 ± 2.32	170.55 ± 1.68	289.85 ± 3.19	296.42 ± 2.67	190.37 ± 2.86	467.50 ± 3.28	368.15 ± 2.61
20	119.52 ± 2.00	125.55 ± 1.54	251.51 ± 2.86	192.95 ± 2.29	160.50 ± 2.69	438.16 ± 3.17	240.33 ± 2.25
Particle size (mm)							
0.5	280.20 ± 2.65	200.13 ± 1.80	320.70 ± 3.02	296.30 ± 2.43	294.64 ± 2.93	398.45 ± 2.97	313.54 ± 2.84
1.0	328.40 ± 2.80	294.18 ± 2.15	500.46 ± 3.73	458.65 ± 2.86	422.03 ± 3.85	511.20 ± 3.90	545.23 ± 3.55
2.0 (control)	276.29 ± 2.47	226.52 ± 1.94	417.23 ± 3.31	360.88 ± 2.94	305.00 ± 3.60	487.16 ± 3.50	475.12 ± 3.31
4.0	204.38 ± 2.81	170.61 ± 1.58	329.73 ± 3.00	312.91 ± 2.64	235.20 ± 3.40	326.49 ± 2.68	368.00 ± 3.16
6.0	129.53 ± 1.82	112.16 ± 1.33	231.44 ± 2.21	183.55 ± 2.17	173.00 ± 2.65	239.72 ± 2.41	325.28 ± 3.00
Initial moisture content (%)							
50	279.38 ± 3.40	136.45 ± 1.57	290.00 ± 3.19	219.71 ± 2.45	212.47 ± 3.00	353.18 ± 2.69	280.41 ± 1.75
60 (control)	328.40 ± 2.80	294.18 ± 2.15	500.46 ± 3.73	458.65 ± 2.86	422.03 ± 3.85	511.20 ± 3.90	545.23 ± 3.55
70	198.40 ± 2.77	195.36 ± 1.70	389.73 ± 3.56	289.59 ± 3.16	242.03 ± 3.46	467.32 ± 3.29	375.23 ± 2.55
80	179.34 ± 2.34	156.86 ± 1.71	250.12 ± 2.42	240.49 ± 2.73	238.65 ± 3.41	398.45 ± 2.97	335.52 ± 2.34
90	162.18 ± 2.50	140.92 ± 1.62	217.55 ± 2.18	226.32 ± 2.51	183.62 ± 2.85	382.70 ± 3.10	290.50 ± 2.22
Temperature (°C)							
25	159.13 ± 2.30	149.69 ± 1.69	243.95 ± 2.37	218.23 ± 2.49	212.47 ± 3.00	398.75 ± 2.90	334.12 ± 2.34
28 (control)	328.40 ± 2.80	294.18 ± 2.15	500.46 ± 3.73	422.03 ± 3.85	422.03 ± 3.85	511.20 ± 3.90	545.23 ± 3.55
32	280.25 ± 3.40	195.90 ± 1.91	390.18 ± 3.56	289.59 ± 3.16	243.18 ± 3.43	467.96 ± 3.29	375.23 ± 2.60
35	198.40 ± 2.77	158.00 ± 1.64	337.63 ± 3.14	260.41 ± 2.97	222.03 ± 3.31	440.67 ± 3.15	284.00 ± 2.29
40	122.56 ± 1.76	130.46 ± 1.56	165.01 ± 1.85	213.20 ± 2.40	185.90 ± 2.71	330.89 ± 2.55	172.13 ± 1.21
45	110.23 ± 1.52	82.70 ± 0.90	98.77 ± 1.06	100.46 ± 1.52	124.18 ± 2.11	250.41 ± 2.21	172.13 ± 1.21
Inoculum size (CFU/gds)							
2×10^6	328.40 ± 2.80	294.18 ± 2.15	500.46 ± 3.73	422.03 ± 3.85	422.03 ± 3.85	511.20 ± 3.90	545.23 ± 3.54
2×10^7	377.90 ± 2.92	358.61 ± 2.83	587.95 ± 4.15	484.95 ± 4.61	498.51 ± 4.17	569.75 ± 3.96	587.00 ± 3.66
2×10^8	298.40 ± 2.47	295.70 ± 2.46	469.15 ± 3.58	390.04 ± 3.17	442.50 ± 3.40	465.20 ± 3.45	398.00 ± 2.87

Table 7
Optimization of SSF process parameters for the productivity of anti-HCV, antioxidant and anticancer by *Arthrinium* sp. FAKSA 10.

SSF Parameter	Anti-hepatitis C virus (IC_{50}; µg/mL)	The antioxidant potential		The anticancer activity IC_{50} (µg/mL)	
		DPPH scavenging activity (IC_{50}; µg/mL)	Reducing Power antioxidant assay (RPAA, $O.D_{700}$)	HepG-2	HCT-116
Incubation period (d)					
5	24.45 ± 1.40	50.00 ± 2.13	0.523	40.88 ± 1.54	60.11 ± 2.50
7	15.29 ± 1.25	24.92 ± 1.81	0.802	28.75 ± 1.89	37.15 ± 1.91
10 (control)	11.22 ± 1.03	11.80 ± 1.19	0.998	10.30 ± 1.04	10.22 ± 1.00
14	28.61 ± 1.49	25.50 ± 1.65	0.798	30.17 ± 1.83	40.50 ± 2.14
20	40.52 ± 1.87	46.22 ± 1.40	0.562	50.49 ± 1.96	54.92 ± 2.28
Particle size (mm)					
0.5	16.85 ± 1.34	35.00 ± 1.90	0.737	29.25 ± 2.17	17.68 ± 1.51
1.0	9.87 ± 0.92	10.00 ± 1.59	1.002	8.75 ± 1.13	9.14 ± 0.93
2.0 (control)	11.22 ± 1.03	11.80 ± 1.40	0.998	10.30 ± 1.08	10.22 ± 1.03
4.0	19.30 ± 1.37	39.45 ± 1.96	0.690	21.17 ± 1.79	15.40 ± 1.39
6.0	28.29 ± 1.46	50.25 ± 2.18	0.517	35.17 ± 2.00	30.91 ± 1.84
Initial moisture content (%)					
50	13.60 ± 1.12	25.58 ± 1.62	0.794	12.00 ± 1.21	17.55 ± 1.50
60 (control)	9.84 ± 0.95	10.04 ± 1.60	1.001	8.77 ± 1.15	9.20 ± 0.95
70	15.33 ± 1.23	19.00 ± 1.37	0.924	17.43 ± 1.62	14.63 ± 1.45
80	21.41 ± 1.34	26.52 ± 1.34	0.786	25.19 ± 1.84	30.55 ± 2.20
90	39.80 ± 1.80	40.86 ± 153	0.685	30.26 ± 1.97	45.70 ± 2.34
Temperature (°C)					
25	17.12 ± 1.30	13.20 ± 1.85	0.945	19.50 ± 0.10	69.00 ± 0.15
28 (control)	9.84 ± 0.95	10.00 ± 1.67	1.000	8.90 ± 1.20	9.18 ± 0.96
32	19.26 ± 1.40	29.36 ± 1.37	0.765	20.16 ± 1.63	24.75 ± 1.25
35	33.00 ± 1.94	46.35 ± 1.55	0.560	50.41 ± 2.33	48.16 ± 2.40
40	52.00 ± 2.15	72.54 ± 2.78	0.500	90.11 ± 2.80	55.14 ± 2.69
45	89.53 ± 2.70	95.70 ± 2.78	0.478	100.72 ± 3.19	78.35 ± 2.92
Inoculum size (CFU/gds)					
2×10^6	9.86 ± 0.96	10.00 ± 1.67	1.080	8.81 ± 1.15	9.20 ± 0.95
2×10^7	8.00 ± 0.85	9.23 ± 1.30	1.110	7.59 ± 1.21	8.12 ± 0.86
2×10^8	18.40 ± 1.37	16.25 ± 1.43	0.916	14.80 ± 1.66	15.13 ± 1.39

arginase, L-glutaminase, and RNase productivity reached a peak (587.95 ± 4.15, 377.90 ± 2.92, 358.61 ± 2.83, 484.95 ± 4.61, 498.5 1 ± 4.17, 569.75 ± 3.96, and 587.00 ± 3.66 U/gds) under the optimized SSF culture conditions of the optimal incubation period; 10 d, particle size; 1 mm, initial moisture content; (60%, v/w); incubation temperature; 28°C, and optimal inoculum size;

(2×10^7 CFU/gds) (Table 6). Likewise, the highest anti-HCV, DPPH scavenging, and anticancer activities were obtained with the lowest IC_{50} (μg/mL) with optimizing the incubation period to 10 d, substrate particle size to 1 mm, initial moisture content to 60%, incubation temperature to 28°C, and inoculum size to 2×10^7 CFU/gds (Table 7). The biosynthesis of products and enzymes with imperative pharmacological and medicinal properties or significant industrial application was reported in certain *Arthrinium* species [56]. The antiviral metabolites targeting HCV which increasing with decreasing IC_{50} values in Table 7 indicated that IC_{50} of anti-HCV metabolites was 11.22 ± 1.03 to 40.52 ± 1.87 μg/mL at incubation period ranged from 5 to 20 d with a peak after incubation for 10 d and ranged from 9.87 ± 0.92 to 28.29 ± 1.46 μg/mL with particle size to 1 mm to 6 mm while it was ranged between 9.84 ± 0.95 and 39.80 ± 1.80 μg/mL with initial moisture content; 50–90% (Table 7). Furthermore, the IC_{50} of anti-HCV metabolites decreased from 17.12 ± 1.30, 19.26 ± 1.40, 33.00 ± 1.94, 52.00 ± 2.15, and 89.53 ± 2.70 μg/mL at 25, 32, 35, 40, and 45°C, respectively, to 9.84 ± 0.95 μg/mL at 28°C as well as from 9.86 ± 0.96, and 18.40 ± 1.37 μg/mL with an inoculum size of 2×10^6 and 2×10^8 to 8.00 ± 0.85 μg/mL with 2×10^7 CFU/gds (Table 7). Antioxidant determined as potential reducing power of antioxidant activity at OD_{700} was increased from 0.523 after 5 d of fermentation to 0.998 on the 10th d of fermentation and then decreased to 0.562 after 20 d of fermentation, and it was increased to 1.002 after reducing the particle size of the substrates from 2 mm to 1 mm while by increasing the inoculum size from 2×10^6 to 2×10^7 CFU/gds was increased to 1.110 (Table 7). Moreover, anti-DPPH radical scavenging capacity was exploited with the lowest IC_{50} (11.80 ± 1.19 μg/mL) with 10 d as the incubation period, 10.00 ± 1.59 μg/mL when substrate was sized to 1 mm and 9.23 ± 1.30 μg/mL with using inoculum size of 2×10^7 CFU/gds (Table 7). In agreement with our results, Bao et al. [57] proposed that marine *Arthrinium* sp. had a pronounced prospective to yield several components that could be the constituents of a wide range of antioxidants, several of which have not been explored until now.

The highest anticancer activity of *Arthrinium* sp. FAKSA 10 metabolites associated with the lowest IC_{50} against the human liver (HepG-2) and colon HCT-116 cancer cells was estimated to be 10.30 ± 1.04 and 10.22 ± 1.00 μg/mL at the 10th d of fermentation, 8.75 ± 1.13; 9.14 ± 0.93 μg/mL with a substrate particle size 1 mm and 8.77 ± 1.15 μg/mL at initial moisture content 60% (Table 7). Furthermore, as shown in Table 7, the IC_{50} of FAKSA 10 extract was decreased after using incubation temperature 28°C (8.90 ± 1.20 and 9.18 ± 0.96 μg/mL) and inoculum size 2×10^7 CFU/gds (7.59 ± 1.21 and 8.12 ± 0.86 μg/mL) against HepG-2 and HCT-116, respectively. Hence, the current investigation suggested using of low-cost abundant resources to produce pharmaceutical enzymes known for their multiple bioactivities including antitumor, antiviral and antioxidant activities. Consistent with our findings, secondary metabolites of endophytic *Arthrinium* species have been recognized as a rich source of anticancer agents such as novel diterpenoids, *Arthrinins* A-D, via cell cycle arrest, modulation of ROS-scavenging enzyme activities, stimulation of apoptosis, as well as suppression of cancer cell proliferation, anti-angiogenic, and anti-metastasis [55].

4. Conclusions

Forty-three endophytic fungal isolates of the marine soft coral *S. polydactyla* grown on wheat bran medium showed high yields of pharmaceutical enzymes including L-glutaminase, L-methioninase, L-arginase, L-asparaginase, L-tyrosinase, L-lysine α-oxidase and ribonuclease. They also showed anti-HCV, antitumor, and antioxidant properties using wheat bran as low-cost medium. Among them, the hyperproducer strain *Arthrinium* sp. FAKSA 10 was selected. Overall, 46 compounds were detected in the extract of *Arthrinium* sp. FAKSA 10 culture on wheat bran medium with a large number of pharmaceutical activities, and then, it is a fit strain for approaching biotechnology. *Arthrinium* sp. FAKSA 10 was able to utilize different agroindustrial residues as fermentation media to produce wide-ranging biologically active metabolites against HCV, and carcinomas of colon and liver along with effective antioxidant activity on DPPH radical scavenging and reducing power assays. Hence, the current work exploited *Arthrinium* sp. FAKSA 10 metabolites as natural pharmaceuticals against cancer and viral diseases along with its notable antioxidant properties revealed in this study. On the other hand, among different residues, oil cakes provide alternative and reliable low-cost media that can improve to produce a high amount of valued bioactive metabolites.

CRediT authorship contribution statement

Mohammad J. Alsarraf: Writing – review & editing, Writing – original draft, Visualization, Validation, Methodology, Investigation, Conceptualization. **Fuad Ameen:** Writing – review & editing, Writing – original draft, Visualization, Validation, Methodology, Investigation, Funding acquisition, Formal analysis, Data curation, Conceptualization. **Abdullah Alfalih:** Writing – review & editing, Writing – original draft, Visualization, Validation, Investigation. **Zirak Sajjad:** Writing – review & editing, Visualization, Validation, Writing – review & editing, Visualization, Validation.

Financial support

This research was funded by Researchers Supporting Project number (RSP2024R364), King Saud University, Riyadh, Saudi Arabia.

Declaration of competing interest

No potential conflict of interest was reported by the authors.

Acknowledgments

Deep thanks and gratitude from the research team to the King Saud University, Riyadh, Saudi Arabia for fund support and assistance of this research work.

Supplementary material

https://doi.org/10.1016/j.ejbt.2024.09.001.

Data availability

Data will be made available on request.

References

[1] Xu J, Yıldıztekin M, Han D, et al. Biosynthesis, characterization, and investigation of antimicrobial and cytotoxic activities of silver nanoparticles using *Solanum tuberosum* peel aqueous extract. Heliyon 2023;9(8):e19061. https://doi.org/10.1016/j.heliyon.2023.e19061.

[2] Awad MF, El-Shenawy FS, El-Gendy MMAA, et al. Purification, characterization, and anticancer and antioxidant activities of L-glutaminase from *Aspergillus versicolor* Faesay4. Int Microbiol 2021;24(2):169–81. https://doi.org/10.1007/s10123-020-00156-8.

[3] Bender D, Koulouri A, Wen X, et al. Guanylate-binding protein 1 acts as a proviral factor for the life cycle of hepatitis C virus. PLoS Pathog 2024;20(2):. https://doi.org/10.1371/journal.ppat.1011976e1011976.

[4] Alghamdi BA, Alhassan AI. The influence of Saudi board of emergency medicine residency educators on residents' academic and clinical performance in Riyadh, Saudi Arabia. Cureus 2024;16(2):e54316. https://doi.org/10.7759/cureus.54316.
[5] El-Bondkly AAM, El-Gendy MMAA, El-Bondkly EAM, et al. Biodiversity and biological activity of fungal microbiota derived from the medicinal plants *Salvia aegyptiaca* L. and *Balanties aegyptiaca* L. Biocatal Agric Biotechnol 2020;28:. https://doi.org/10.1016/j.bcab.2020.101720101720.
[6] Asomadu RO, Ezeorba TPC, Ezike TC, et al. Exploring the antioxidant potential of endophytic fungi: A review on methods for extraction and quantification of total antioxidant capacity (TAC). 3Biotech 2024;14(5):127. https://doi.org/10.1007/s13205-024-03970-3.
[7] Costa M, Silva TA, Guimarães DSP. The recombinant L-lysine α-oxidase from the fungus *Trichoderma harzianum* promotes apoptosis and necrosis of leukemia CD34 + hematopoietic cells. Microb Cell Fact 2024;23:51. https://doi.org/10.1186/s12934-024-02315-2.
[8] Alzahrani NH, El-Bondkly AAM, El-Gendy MMAA, et al. Enhancement of undecylprodigiosin production from marine endophytic recombinant strain *Streptomyces* sp. ALAA-R20 through low-cost induction strategy. J Appl Genetics 2021;62(1):165–82. https://doi.org/10.1007/s13353-020-00597-x.
[9] El-Gendy MMA, Awad MF, El-Shenawy FS, et al. Production, purification, characterization, antioxidant and antiproliferative activities of extracellular L-asparaginase produced by *Fusarium equiseti* AHMF4. Saudi J Biol Sci 2021;28 (4):2540–8. https://doi.org/10.1016/j.sjbs.2021.01.058.
[10] Hoang PT, Luong QXT, Ayun RQ, et al. A novel approach of antiviral drugs targeting viral genomes. Microorganisms 2022;10(8):1552. https://doi.org/10.3390/microorganisms10081552.
[11] Li J, Boix E. Host defence RNases as antiviral agents against enveloped single stranded RNA viruses. Virulence 2021;12(1):444–69. https://doi.org/10.1080/21505594.2021.1871823.
[12] El-Gendy MMAA, Yahya SMM, Hamed AR, et al. Phylogenetic analysis and biological evaluation of marine endophytic fungi derived from Red Sea sponge *Hyrtios erectus*. Appl Biochem Biotechnol 2018;185:755–77. https://doi.org/10.1007/s12010-017-2679-x.
[13] Pokrovsky VS, Chepikova OE, Davydov DZ, et al. Amino acid degrading enzymes and their application in cancer therapy. Curr Med Chem 2019;26 (3):446–64. https://doi.org/10.2174/0929867324666171006132729.
[14] Nadaf P, Kulkarni AG, Vedamurthy A. Isolation, screening and characterization of L-arginase producing soil bacteria. Int J Pharm Sci Res 2019;10(7):3440–4. https://doi.org/10.13040/IJPSR.0975-8232.10(7).3440-44.
[15] Lukasheva EV, Babayeva G, Karshieva SS, et al. L-lysine α-oxidase: Enzyme with anticancer properties. Pharmaceuticals 2021;14(11):1070. https://doi.org/10.3390/ph14111070.
[16] El-Gendy MMAA, Al-Zahrani SH, El-Bondkly AMA. Construction of potent recombinant strain through intergeneric protoplast fusion in endophytic fungi for anticancerous enzymes production using rice straw. Appl Biochem Biotechnol 2017;183:30–50. https://doi.org/10.1007/s12010-017-2429-0.
[17] Pintos A, Alvarado P, Planas J, et al. Six new species of *Arthrinium* from Europe and notes about *A. caricicola* and other species found in *Carex* spp. Hosts Mycokeys 2019;49:15–48. https://doi.org/10.3897/mycokeys.49.32115.
[18] Swathi AV, Dhanalakshmi SV. Optimization of process parameters for L-methioninase production in solid state fermentation by *Aspergillus flavipes* from sesame oil cake. Euro J Biotechnol Biosci 2015;3:16–21.
[19] El-Bondkly AAM, El-Gendy MMAA, El-Bondkly AMA. Construction of efficient recombinant strain through genome shuffling in marine endophytic *Fusarium* sp. ALAA-20 for improvement lovastatin production using agro-industrial wastes. Arab J Sci Eng 2021;46(1):175–90. https://doi.org/10.1007/s13369-020-04925-5.
[20] Abdel-Hamid NS, Abdel-Khaleka HH, El-Shahat RM, et al. Optimization of L-asparaginase production from *Fusarium oxysporum* F-S3 using irradiated pomegranate peel under solid-state fermentation. Egypt J Chem 2022;65 (6):381–97. https://doi.org/10.21608/ejchem.2021.104129.4817.
[21] Javia BM, Gadhvi MS, Vyas SJ, et al. Bioprospecting of a thermostable L-methioninase from *Alcaligenes aquatilis* BJ-1 in agro-industrial waste. Microbiol Res 2023;14(3):959–76. https://doi.org/10.3390/microbiolres14030066.
[22] Heo YM, Kim K, Ryu SM, et al. Diversity and ecology of marine algicolous *Arthrinium* species as a source of bioactive natural products. Mar Drugs 2018;16(12):508. https://doi.org/10.3390/md16120508.
[23] El-Gendy MMA, El-Bondkly AM. Production and genetic improvement of a novel antimycotic agent, saadamycin, against dermatophytes and other clinical fungi from endophytic *Streptomyces* sp. Hedaya48. J Industrial Microbiol Biotechnol 2010;37:831–41. https://doi.org/10.1007/s10295-010-0729-2.
[24] Dalfard AB, Khajeh K, Soudi MR, et al. Isolation and biochemical characterization of laccase and tyrosinase activities in a novel melanogenic soil bacterium. Enzyme Microb Technol 2006;39(7):1409–16. https://doi.org/10.1016/j.enzmictec.2006.03.029.
[25] Wu Y, Wang H, Ng T. Purification and characterization of a novel RNase with antiproliferative activity from the mushroom *Lactarius flavidulus*. J Antibiot 2012;65:67–72. https://doi.org/10.1038/ja.2011.112.
[26] El-Gendy MMA, El-Bondkly AMA, Yahya SMM. Production and evaluation of antimycotic and antihepatitis C virus potential of fusant MERV6270 derived from mangrove endophytic fungi using novel substrates of agroindustrial wastes. Appl Biochem Biotechnol 2014;174:2674–701. https://doi.org/10.1007/s12010-014-1218-2.
[27] Munsell Color. Munsell soil-color charts with genuine Munsell color chips. Munsell Color, Grand Rapids, 2009; MI, USA.
[28] Hughes SJ. Conidiophores, conidia, and classification. Can J Bot 1953;31:577–659. https://doi.org/10.1139/b53-046.
[29] Minter DW. A re-appraisal of the relationships between *Arthrinium* and other hyphomycetes. Proc Indian Acad Sci 1985;94:281–308. https://doi.org/10.1007/BF03053145.
[30] Cole GT. Models of cell differentiation in conidial fungi. Microbiol Rev 1986;50:95–132. https://doi.org/10.1128/MMBR.50.2.95-132.1986.
[31] Wang M, Tan XM, Liu F, et al. Eight new *Arthrinium* species from China. MycoKeys 2018;34:1–24. https://doi.org/10.3897/mycokeys.34.24221.
[32] White TJ, Bruns T, Lee S. Amplification and direct sequencing of fungal ribosomal RNA genes for phylogenetics. In: Innis MA, Gelfand DH, Sninsky JJ, White TJ, editors. PCR protocols: A guide to methods and applications. New York: Academic Press, Inc.; 1990. p. 315–22. https://doi.org/10.1016/B978-0-12-372180-8.50042-1.
[33] El-Bondkly AMA. Molecular identification using ITS sequences and genome shuffling to improve 2-deoxyglucose tolerance and xylanase activity of marine-derived fungus, *Aspergillus* sp. NRCF5. Appl Biochem Biotechnol 2012;167:2160–73. https://doi.org/10.1007/s12010-012-9763-z.
[34] Kumar S, Stecher G, Li M, et al. MEGA X: Molecular evolutionary genetics analysis across computing platforms. Mol Biol Evol 2018;35:1547–9. https://doi.org/10.1093/molbev/msy096.
[35] Tamura K, Stecher G, Kumar S. MEGA 11: Molecular evolutionary genetics analysis version 11. Mol Biol Evol 2021;38(7):3022–7. https://doi.org/10.1093/molbev/msab120.
[36] Tamura K, Nei M, Kumar S. Prospects for inferring very large phylogenies by using the neighbor-joining method. Proc Natl Acad Sci 2004;101(30):11030–5. https://doi.org/10.1073/pnas.0404206101.
[37] van Meerloo J, Kaspers GJ, Cloos J. Cell sensitivity assays: The MTT assay. Methods Mol Biol 2011;731:237–45. https://doi.org/10.1007/978-1-61779-080-5_20.
[38] Makris DP, Psarra E, Kallithraka S, et al. The effect of polyphenolic composition as related to antioxidant capacity in white wines. Food Res Int 2003;36 (8):805–14. https://doi.org/10.1016/S0963-9969(03)00075-9.
[39] Hue SM, Boyce AN, Somasundram C. Antioxidant activity, phenolic and flavonoid contents in the leaves of different varieties of sweet potato (*Ipomoea batatas*). Aust J Crop Sci 2012;6:375–80.
[40] Lukasheva EV, Makletsova MG, Lukashev AN, et al. Fungal enzyme L-lysine α-oxidase affects the amino acid metabolism in the brain and decreases the polyamine level. Pharmaceuticals 2020;13(11):398. https://doi.org/10.3390/ph13110398.
[41] Lopez-Tejedor D, Claveria-Gimeno R, Velazquez-Campoy A, et al. *In vitro* antiviral activity of tyrosinase from mushroom *Agaricus bisporus* against hepatitis C virus. Pharmaceuticals 2021;14(8):759. https://doi.org/10.3390/ph14080759.
[42] Javia BM, Gadhvi MS, Vyas SJ, et al. A review on L-methioninase in cancer therapy: Precision targeting, advancements and diverse applications for a promising future. Int J Biol Macromol 2024;265(Pt 2):. https://doi.org/10.1016/j.ijbiomac.2024.130997130997.
[43] Vineetha MS, Aldabaan NA, More SS, et al. Production and optimization of L-glutaminase from halophilic *Fusarium solani-melongenae* strain CRI 24 under submerged and solid state fermentation. J Pure Appl Microbiol 2024;18 (1):593–604. https://doi.org/10.22207/JPAM.18.1.43.
[44] Li S, Yu Y, Xie P, et al. Antifungal activities of L-methionine and L-arginine treatment *in vitro* and *in vivo* against *Botrytis cinerea*. Microorganisms 2024;12 (2):360. https://doi.org/10.3390/microorganisms12020360.
[45] Gotte G, Menegazzi M. Biological activities of secretory RNases: Focus on their oligomerization to design antitumor drugs. Front Immunol 2019;10:2626. https://doi.org/10.3389/fimmu.2019.02626.
[46] Burrack KS, Morrison TE. The role of myeloid cell activation and arginine metabolism in the pathogenesis of virus-induced diseases. Front Immunol 2014;5:428. https://doi.org/10.3389/fimmu.00428.
[47] Srivastava A, Srivastava AK, Vishwkarma A, et al. Synthesis, spectroscopic studies and biological aspects of bis (cyclopentadienyl) titanium (IV) complexes with 4-amino-5-(nicotinic/picolinic/isonicotinic/indole-3-propyl/indole-3-ethyl)-3-mercapto-1,2,4-triazole. J Indian Chem Soc 2020;97 (11b):2363–71.
[48] El-Sayed ER, Hazaa MA, Shebl MM, et al. Bioprospecting endophytic fungi for bioactive metabolites and use of irradiation to improve their bioactivities. AMB Express 2022;12(1):46. https://doi.org/10.1186/s13568-022-01386-x.
[49] Dandash F, Leger DY, Diab-Assaf M, et al. Porphyrin/chlorin derivatives as promising molecules for therapy of colorectal cancer. Molecules 2021;26 (23):7268. https://doi.org/10.3390/molecules26237268.
[50] Morland C, Nordengen K. N-Acetyl-aspartyl-glutamate in brain health and disease. Int J Mol Sci 2022;23(3):1268. https://doi.org/10.3390/ijms23031268.
[51] Stradiotto A, Kosoko-Lasaki S. Glaucoma pharmacology. In: Sunny EO, Najam AS (editors), Handbook of Basic and Clinical Ocular Pharmacology and Therapeutics, 2022; Academic Press, Elsevier Inc. https://doi.org/10.1016/B978-0-12-819291-7.00008-3.
[52] Crous PW, Groenewald JZ. A phylogenetic re-evaluation of *Arthrinium*. IMA Fungus 2013;4:133–54. https://doi.org/10.5598/imafungus.2013.04.01.13.
[53] Elissawy AM, Ebada SS, Ashour ML, et al. Spiroarthrinols A and B, two novel meroterpenoids isolated from the sponge-derived fungus *Arthrinium* sp.

Phytochem Lett 2017;20:246–51. https://doi.org/10.1016/j.phytol.2017.05.008.
[54] Shu Y, Wang JP, Li BX, et al. Bioactive cytochalasans from the fungus *Arthrinium arundinis* DJ-13. Phytochemistry 2022;194:. https://doi.org/10.1016/j.phytochem.2021.113009113009.
[55] Ebada SS, Schulz B, Wray V, et al. *Arthrinins* A-D: Novel diterpenoids and further constituents from the sponge derived fungus *Arthrinium* sp. Bioorg Med Chem 2011;19(15):4644–51. https://doi.org/10.1016/j.bmc.2011.06.013.
[56] Hong JH, Jang S, Heo YM, et al. Investigation of marine-derived fungal diversity and their exploitable biological activities. Mar Drugs 2015;13:4137–55. https://doi.org/10.3390/md13074137.
[57] Bao J, He F, Yu JH, et al. New chromones from a marine-derived fungus, *Arthrinium* sp., and their biological activity. Molecules 2018;23(8):1982. https://doi.org/10.3390/molecules23081982.